PB84-151224

Improved Techniques for Residual Ozone

Miami Univ., Oxford, OH

Prepared for

Municipal Environmental Research, Cincinnati, OH

Jan 84

U.S. Department of Commerce
National Technical Information Service
NTIS

EPA-600/2-84-036
January 1984

PB84-151224

IMPROVED TECHNIQUES FOR RESIDUAL OZONE

by

Gilbert Gordon
Joyce F. Grunwell
Department of Chemistry
Miami University
Oxford, Ohio 45056

Cooperative Agreement CR806302

Project Officer

Edward J. Opatken
Wastewater Research Division
Municipal Environmental Research Laboratory
Cincinnati, Ohio 45268

REPRODUCED BY
NATIONAL TECHNICAL
INFORMATION SERVICE
U.S. DEPARTMENT OF COMMERCE
SPRINGFIELD, VA. 22161

MUNICIPAL ENVIRONMENTAL RESEARCH LABORATORY
OFFICE OF RESEARCH AND DEVELOPMENT
U.S. ENVIRONMENTAL PROTECTION AGENCY
CINCINNATI, OHIO 45268

BEGIN FIRST LINE OF TEXT HERE
CENTER OF PAGE
TOP OF IMAGE AREA
DROPPED HEAD, BEGIN SECTIONS HERE
0.1/2"
0.1/8"
BEGIN LAST LINE OF TEXT
3/8"
BOTTOM OF IMAGE AREA, OUTSIDE DIMENSION FOR TABLES AND ILLUSTRATIONS
PAGE NUMBER
EPA Form 2350-4 (4-80)
(PREVIOUSLY CIN. EPA FORM 287)
TYPING GUIDE SHEET

TECHNICAL REPORT DATA (Please read Instructions on the reverse before completing)		
1. REPORT NO. EPA-600/2-84-036	2.	3. RECIPIENT'S ACCESSION NO. PB84 151224
4. TITLE AND SUBTITLE Improved Techniques for Residual Ozone		5. REPORT DATE January 1984 6. PERFORMING ORGANIZATION CODE
7. AUTHOR(S) G. Gordon J. F. Grunwell		8. PERFORMING ORGANIZATION REPORT NO.
9. PERFORMING ORGANIZATION NAME AND ADDRESS Department of Chemistry Miami University Oxford, Ohio 45056		10. PROGRAM ELEMENT NO. PE CAZB1B, DU B113, A/20 11. CONTRACT/GRANT NO. CA CR806302
12. SPONSORING AGENCY NAME AND ADDRESS Municipal Environmental Research Laboratory-Cinti, OH Office of Research and Development U.S. Environmental Protection Agency Cincinnati, Ohio 45268		13. TYPE OF REPORT AND PERIOD COVERED 14. SPONSORING AGENCY CODE EPA/600/14
15. SUPPLEMENTARY NOTES Project Officer: Edward J. Opatken (513) 684-7643		

16. ABSTRACT Eight analytical methods for the determination of residual ozone in water are evaluated. Four are iodometric methods based on the reduction of ozone by iodide ion: the iodometric method, the amperometric method, the arsenic (III) back titration method, and the N, N-diethyl-p-phenylenediamine (DPD) method. Four are non-iodometric methods: the indigo method, the arsenic (III) direct oxidation method, the Delta electrode, and the direct measurement of ultraviolet absorption at 259 nm. Two or more analytical methods are compared by simultaneous measurement of the decay curve of ozone in water. This kinetic technique allows a direct comparison of methods under conditions of rapidly changing ozone concentration. The mechanism of ozone decay is discussed.

The eight analytical methods are compared on ease of calibration of the reagent solutions, the stability of the reagent solutions, the stability of the concentration of the ozonated reagent solutions, and the validity of the ozone concentration. No iodometric method is recommended. The Delta electrode failed to maintain calibration and failed to respond linearly over a 10 mg/l ozone range. The indigo method and the arsenic (III) direct oxidation method are the methods of choice.

Four exploratory methods based on new ozone-reductant reactions are discussed: the chlorite ion method, the iodate method, the iron (II) terpyridine method, and the cerium method. The failure of these potential new methods is traced.

17. KEY WORDS AND DOCUMENT ANALYSIS		
a. DESCRIPTORS	b. IDENTIFIERS/OPEN ENDED TERMS	c. COSATI Field/Group
Disinfection, Disinfectants, Ozone, Ozonation, Wastewater	Ozone contactors	13B 06M
18. DISTRIBUTION STATEMENT Release to Public	19. SECURITY CLASS (This Report) Unclassified 20. SECURITY CLASS (This page) Unclassified	21. NO. OF PAGES 90 22. PRICE

EPA Form 2220-1 (9-73)

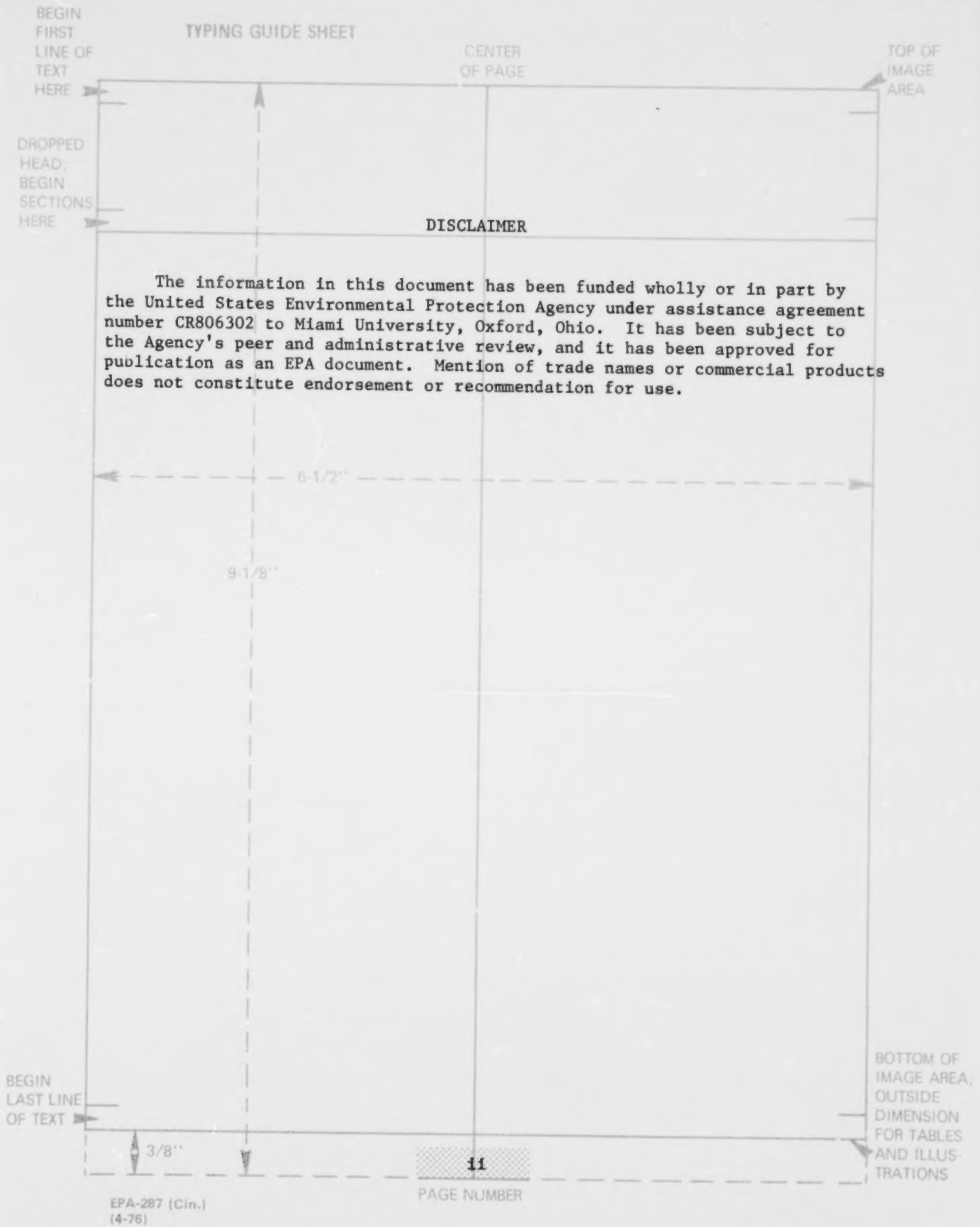

DISCLAIMER

The information in this document has been funded wholly or in part by the United States Environmental Protection Agency under assistance agreement number CR806302 to Miami University, Oxford, Ohio. It has been subject to the Agency's peer and administrative review, and it has been approved for publication as an EPA document. Mention of trade names or commercial products does not constitute endorsement or recommendation for use.

EPA-287 (Cin.)
(4-76)

FOREWORD

The U.S. Environmental Protection Agency was created because of increasing public and government concern about the dangers of pollution to the health and welfare of the American people. Noxious air, foul water, and spoiled land are tragic testimonies to the deterioration of our natural environment. The complexity of that environment and the interplay of its components require a concentrated and integrated attack on the problem.

Research and development is that necessary first step in problem solution, and it involves defining the problem, measuring its impact, and searching for solutions. The Municipal Environmental Research Laboratory develops new and improved technology and systems to prevent, treat, and manage wastewater and solid and hazardous waste pollutant discharges from municipal and community sources, to preserve and treat public drinking water supplies, and to minimize the adverse economic, social, health, and aesthetic effects of pollution. This publication is one of the products of that research and is a most vital communication link between the researcher and the user community.

This report on the various analytical techniques that have been used in determining ozone residuals was needed to establish a reliable method. The users of ozone disinfection can now employ methods that accurately determine ozone residuals and can potentially reduce costs by reducing the applied ozone dosage.

Francis T. Mayo
Director
Municipal Environmental Research
Laboratory

BEGIN FIRST LINE OF TEXT HERE
CENTER OF PAGE
TOP OF IMAGE AREA
DROPPED HEAD: BEGIN SECTIONS HERE
BEGIN LAST LINE OF TEXT
3/8"
BOTTOM OF IMAGE AREA; OUTSIDE DIMENSION FOR TABLES AND ILLUSTRATIONS
PAGE NUMBER
EPA Form 2350-4 (4-80)
(PREVIOUSLY CIN, EPA FORM 287)
TYPING GUIDE SHEET

BEGIN FIRST LINE OF TEXT HERE
CENTER OF PAGE
TOP OF IMAGE AREA
DROPPED HEAD; BEGIN SECTIONS HERE

ABSTRACT

Eight analytical methods for the determination of residual ozone in water are evaluated. Four are iodometric methods based on the reduction of ozone by iodide ion: the iodometric method, the amperometric method, the arsenic(III) back titration method, and the N,N-diethyl-p-phenylenediamine (DPD) method. Four are non-iodometric methods: the indigo method, (based on reduction by a carbon-carbon double bond), the arsenic(III) direct oxidation method, the Delta electrode, and the direct measurement of ultraviolet absorption at 259 nm. Two or more analytical methods are compared by simultaneous measurement of the decay curve of ozone in water. This kinetic technique minimizes sampling errors resulting from concentration changes and allows a direct comparison of methods under conditions of rapidly changing ozone concentration. Changes in the ozone-reductant reaction cause differences in ozone decay curves. Differences between iodometric and non-iodometric methods are not directly caused by iodate ion formation or hydrogen peroxide formation. Differences between methods are reduced by conditions that minimize ozone decay before its reaction by reductant. Ozone decay is slowed by decreasing pH, increasing concentration of radical scavengers, and increasing concentration of specific anions such as phosphate ions and carbonate ions. The mechanism of ozone decay is discussed.

The eight analytical methods are compared on ease of calibration of the reagent solutions, the stability of the reagent solutions, the stability of the concentration of the ozonated reagent solutions, and the validity of the ozone concentration. No iodometric method is recommended. The Delta electrode failed to maintain calibration and failed to respond linearly over a 10 mg/L ozone range. The indigo method and the arsenic(III) direct oxidation method are the methods of choice. Even these methods occasionally give a point 30%-50% removed from that calculated on an otherwise smooth decay curve. This makes single point residual ozone analyses untrustworthy.

Four exploratory methods based on new ozone-reductant reactions are discussed: the chlorite ion method, the iodate method, the iron(II) terpyridine method, and the cerium method. The failure of these potential new methods is traced.

This report was submitted in fulfillment of Grant No. R 806302010 by Miami University under the sponsorship of the U.S. Environmental Protection Agency. This report covers the period December 11, 1978 to March 10, 1982 and all work was completed as of June 1, 1982.

BEGIN LAST LINE OF TEXT
BOTTOM OF IMAGE AREA; OUTSIDE DIMENSION FOR TABLES AND ILLUSTRATIONS
3/8"

EPA Form 2350-4 (4-80)
(PREVIOUSLY CIN. EPA FORM 287)
© U.S. GOVERNMENT PRINTING OFFICE 1981-560-059
TYPING GUIDE SHEET

BEGIN FIRST LINE OF TEXT HERE
CENTER OF PAGE
TOP OF IMAGE AREA
DROPPED HEAD: BEGIN SECTIONS HERE

CONTENTS

Foreword iii

Abstract iv

Figures vii

Tables ix

Acknowledgments xi

1. Introduction 1

2. Conclusions and Recommendations 3

3. Literature Background 5

4. Experimental Procedures 14

5. Results and Discussion 28

Method Comparisons 28

Iodate Ion Formation 34

Hydrogen Peroxide Formation 36

Buffer Effects 37

Causes for Method Differences 37

Hydrogen Peroxide Effect 40

Ozone Decay 41

Purging Technique 43

Delta Electrode 44

Ozone Decay in Waste Water 47

6-1/2"
9-1/8"
BEGIN LAST LINE OF TEXT
BOTTOM OF IMAGE AREA OUTSIDE DIMENSION FOR TABLES AND ILLUSTRATIONS
3/8"
PAGE NUMBER
EPA Form 2350-4 (4-80)
(PREVIOUSLY CIN, EPA FORM 267)
U.S. GOVERNMENT PRINTING OFFICE 1981-520-159
TYPING GUIDE SHEET

New Reductant Systems 49

Chlorite Ion Method 49

Iron(II) Terpyridine Method 57

Iodate Method 66

Cerium Method 71

References 75

BEGIN FIRST LINE OF TEXT HERE
CENTER OF PAGE
TOP OF IMAGE AREA
DROPPED HEAD: BEGIN SECTIONS HERE
6-1/2"
9-1/8"
BEGIN LAST LINE OF TEXT
3/8"
PAGE NUMBER
BOTTOM OF IMAGE AREA OUTSIDE DIMENSION FOR TABLES AND ILLUSTRATIONS
EPA Form 2350-4 (4-80)
(PREVIOUSLY CIH. EPA FORM 287)
TYPING GUIDE SHEET

FIGURES

Number		Page
1.	The DPD Method	8
2.	Contactor with Flow Cell	15
3.	Water Jacketed Contactor	15
4.	Multi-Stop Calibrated Syringe	17
5.	One Stop Calibrated Syringe	17
6.	UV Visible Spectrum of DPD	19
7.	Stability of Ozone Titer for DPD	19
8.	Stability of Ozone Titer for As(III) Back Titration	22
9.	Stability of Ozone Titer for Indigo	22
10.	Stability of Ozone Titer for As(III) Direct Oxidation	23
11.	Comparison of As(III) and PAO as Direct Reductants	29
12.	Comparison of DPD and As(III) Back Titration in Purified Water	31
13.	Comparison of DPD and As(III) Back Titration in Purified Water with 4.8 mg/L H_2O_2	31
14.	Comparison of DPD and As(III) Back Titration in Tap Water	32
15.	Comparison of DPD and Indigo in Purified Water	32
16.	Comparison of Indigo and As(III) Back Titration in Phosphate Buffer pH 7.21	35
17.	Comparison of UV, Indigo and As(III) Back Titration in Phosphate Buffer pH 7.2	35
18.	Comparison of Indigo, As(III) Back, and As(III) Direct in Phosphate Buffer pH 6.7 : Ozone 30 min	38
19.	Comparison of Indigo, As(III) Back, and As(III) Direct in Phosphate Buffer pH 6.7 : Ozone 60 min	38

BEGIN FIRST LINE OF TEXT HERE
CENTER OF PAGE
TOP OF IMAGE AREA
DROPPED HEAD: BEGIN SECTIONS HERE
BEGIN LAST LINE OF TEXT
3/8"
BOTTOM OF IMAGE AREA; OUTSIDE DIMENSION FOR TABLES AND ILLUSTRATIONS
PAGE NUMBER
EPA Form 2350-4 (4-80)
(PREVIOUSLY CIN, EPA FORM 287)
TYPING GUIDE SHEET

20. Comparison of Indigo, As(III) Direct, and UV in Phosphate Buffer pH 7.7 39

21. Comparison of UV, As(III) Direct, and Indigo in Phosphoric Acid pH 2.3 39

22. Comparison of UV, As(III) Direct (pH 4.5 acetate) and As(III) Direct (pH 6.8 phosphate) in Purified Water 42

23. Effect of pH on Ozone Decay in Phosphate Buffers 42

24. Comparison of UV, Indigo and Delta Electrode in Purified Water 48

25. Comparison of Indigo, Delta Electrode, As(III) Back and As(III) Direct in Waste Water 48

26. Ozone Decay in Waste Water Following Three Sequential Ozone Treatments 50

27. Ozone Decay in Waste Water Following Five Sequential Ozone Treatments 50

28. Comparison of As(III) Back, DPD, and Chlorite Ion in Purified Water 56

29. Comparison of As(III) Back, DPD, and Chlorite Ion in Tap Water 56

30. Calibration Curve for $Fe(terpy)_2^{+2}$ 60

31. Calibration Curve for $Fe(phen)_3^{+2}$ 60

32. Calibration Curve for $Fe(bipy)_3^{+2}$ 61

33. Competitive Reaction of Ozone with $Fe(terpy)_2^{+2}$ and As(III) 61

34. Comparison of As(III) Direct and $Fe(terpy)_2^{+2}$ in Purified Water 65

35. Comparison of DPD, $Fe(terpy)_2^{+2}$, and As(III) Back in Purified Water 65

36. Hydrogen Peroxide Analysis by the Cerium Method 73

37. Comparison of DPD, As(III) Back, and Cerium(III) in Purified Water 74

38. Comparison of DPD, As(III) Back, and Cerium(III) in Tap Water 74

BEGIN FIRST LINE OF TEXT HERE
CENTER OF PAGE
TOP OF IMAGE AREA
DROPPED HEAD, BEGIN SECTIONS HERE
BEGIN LAST LINE OF TEXT
3/8"
BOTTOM OF IMAGE AREA; OUTSIDE DIMENSION FOR TABLES AND ILLUSTRATIONS
PAGE NUMBER
EPA Form 2350-4 (4-80)
(PREVIOUSLY CIN. EPA FORM 287)
TYPING GUIDE SHEET

TABLES

Number		Page
1.	Iodometric Methods for Ozone Analysis	9
2.	Non-Iodometric Methods for Ozone Analysis	9
3.	Stability of Ozone in Water at pH 2	20
4.	Decomposition of Indigo Disulfonate Stock Solutions	21
5.	Decomposition of Indigo Trisulfonate Stock Solutions	21
6.	Weight Preparations for Iron(II) Indicator Solutions	25
7.	Comparison of Experimental and Calculated Ozone Concentration for Inorganic As(III) as Direct Reductant	29
8.	Comparison of PAO and Sodium Thiosulfate in the Amperometric Method Along with a Comparison of the Amperometric Method with As(III) Direct Oxidation	30
9.	Iodometric (pH 3.5 - 9.0) vs. As(III) Direct (pH 7.0)	33
10.	Comparison of Iodometric Method and Arsenic(III) Direct Oxidation	33
11.	Iodate Ion Formation	34
12.	Iodate Ion Formation pH 7	36
13.	Hydrogen Peroxide Formation with Ozone Decay	36
14.	Effect of UV on Hydrogen Peroxide Formation with Ozone Decay	36
15.	Effect of Hydrogen Peroxide on Concentration of Residual Ozone	40
16.	Comparison of Buffers for As(III) Direct Reduction	41
17.	Effect of Phosphate and Carbonate Ions on Ozone Decay	41
18.	Evaluation of the Purging Technique with the Indigo Method on Acid Stabilized Ozone Solutions	43
19.	Evaluation of the Purging Technique with the Indigo Method on Acid Stabilized Ozone Solutions	44

BEGIN FIRST LINE OF TEXT HERE
CENTER OF PAGE
TOP OF IMAGE AREA
DROPPED HEAD: BEGIN SECTIONS HERE
BEGIN LAST LINE OF TEXT
3/8"
BOTTOM OF IMAGE AREA OUTSIDE DIMENSION FOR TABLES AND ILLUSTRATIONS
PAGE NUMBER
EPA Form 2350-4 (4-80)
(PREVIOUSLY CIN. EPA FORM 287)
TYPING GUIDE SHEET

20. Electrode 1. Dilution Experiment 1 for Linear Response . . . 45

21. Electrode 1. Dilution Experiment 2 for Linear Response . . . 45

22. Electrode 1. Dilution Experiment 3 for Linear Response . . . 46

23. Electrode 2. Dilution Experiment 4 for Linear Response . . . 46

24. Electrode 1. Calibration Stability of the Delta Electrode. . 47

25. Effect of Chlorite Ion Concentration on Chlorine Dioxide Formation 51

26. Effect of pH on Chlorine Dioxide Formation 52

27. Decomposition of Chlorite Ion in 2×10^{-1} M Acetate Buffer. . 53

28. Reaction Between Chlorine Dioxide and Ozone 53

29. Reaction Between Chlorine Dioxide and Hydrogen Peroxide . . . 54

30. Determination of Residual Ozone by Chlorite Ion and by Chlorine Dioxide 55

31. Properties of Iron(II) Chelates 58

32. Stability of Absorbance Reading for $Fe(terpy)_2^{+2}$ Method . . . 62

33. Oxidation of Iron(II) Complexes by Cerium(IV) 63

34. Properties of Ruthenium(II) Complexes 64

35. Kinetic Comparison of Iodometric and Iodate Methods 67

36. Effect of Hydroxide Ion on the Disproportionation of Iodine to Iodate Ion 69

37. Effect of Carbonate and Phosphate Ions on the Disproportionation of Iodine 69

38. Effect of Carbonate Ion on the Disproportionation of Iodine 70

39. Effect of Iodide Ion on the Disproportionation of Iodine . . 70

40. Effect of Reaction Time on the Disproportionation of Iodine 71

EPA Form 2350-4 (4-80)
(PREVIOUSLY CIN. EPA FORM 287)
TYPING GUIDE SHEET

ACKNOWLEDGMENTS

Sincere thanks are extended to the following individuals who were involved in this project and who contributed significantly to its completion.

Joseph Benga, Ph.D. - Ph.D. Miami University
Harry Cohen, M.S. - M.S. Miami University
Dwight Emerich, Ph.D. - Ph.D. Miami University
Barbara Thomas - B.S. candidate, Miami University
Hiroshi Tomiyasu, Ph.D. - Post-Doctoral Research Associate on leave from Shinshu University, Matsumoto, Japan

BEGIN FIRST LINE OF TEXT HERE
CENTER OF PAGE
TOP OF IMAGE AREA
DROPPED HEAD BEGIN SECTIONS HERE
BEGIN LAST LINE OF TEXT
BOTTOM OF IMAGE AREA, OUTSIDE DIMENSION FOR TABLES AND ILLUSTRATIONS
PAGE NUMBER
EPA Form 2350-4 (4-80)
(PREVIOUSLY CIN- EPA FORM 287)
U.S. GOVERNMENT PRINTING OFFICE 1981/960-009
TYPING GUIDE SHEET

BEGIN FIRST LINE OF TEXT HERE
CENTER OF PAGE
TOP OF IMAGE AREA
DROPPED HEAD; BEGIN SECTIONS HERE

SECTION 1

INTRODUCTION

In the past eighty years, chlorine has been widely used for disinfection of municipal and industrial wastewaters. But recent concerns over the toxic effects of chlorinated organic byproducts produced during chlorination of potable water and wastewater have renewed interest in the use of ozone for water treatment. In addition to serving as an effective disinfectant ozone acts as an oxidant to remove taste, color, odor, and organic matter from water. The U.S. Environmental Protection Agency (EPA) requires that the residual of any disinfectant be measured accurately and conveniently. In the case of ozone, the residual may vary from 0.1 mg/L to 30 mg/L depending on reaction time, sample contamination, and dosage level. Residual ozone levels below 5 mg/L are typical in water and wastewater treatment (1).

Ozone is an extremely strong oxidizing agent with a standard reduction potential of 2.07V in acid solution and 1.24V in basic solution.

$$O_3 + 2H^+ + 2e^- \rightarrow O_2 + H_2O \qquad E^\circ = 2.07V$$

$$O_3 + H_2O + 2e^- \rightarrow O_2 + 2OH^- \qquad E^\circ = 1.24V$$

Ozone will react with most oxidizable substances, it is a sparingly soluble gas that decomposes in aqueous solution. The rate of decomposition can vary from slow (half-life ($t_{1/2}$) = 10 hours) to fast ($t_{1/2}$ = 100 sec), depending on experimental conditions.

Ozone is usually generated by passing a stream of dry oxygen through an electrical discharge that converts 2% to 5% of the oxygen to ozone.

Ideally methods for determining residual ozone should be verified by the analysis of weighed samples of pure ozone. Such a procedure is impossible, however, because of the instability of pure ozone, the low solubility of ozone in water, the high volatility of ozone, and the rapid decomposition of ozone in water.

A number of analytical methods for determining aqueous ozone have been described in the literature. Most of these methods depend on the strong oxidizing property of ozone. Some of the most popular reductants are iodide ion (2), inorganic arsenic(III), phenylarsine oxide (PAO), which is an organic analogue of arsenic(III) (3), and the dye indigo blue (4). An amperometric

BEGIN LAST LINE OF TEXT
3/8"
BOTTOM OF IMAGE AREA; OUTSIDE DIMENSION FOR TABLES AND ILLUSTRATIONS

EPA Form 2350-4 (4-80)
(PREVIOUSLY CIN: EPA FORM 287)
TYPING GUIDE SHEET

membrane electrode, operating at a potential where only very strong oxidants are reduced, measures ozone in solution (5). This project compares and evaluates these published analytical methods.

In addition, alternative reductants for ozone were investigated over the course of this project in attempts to develop new and improved analytical methods for ozone. The objective was to discover a reductant system that would be selective for very strong oxidants such as ozone, that would produce a stable ozone titer, and that would require minimum instrumentation. The systems we explored were chlorite/chlorine dioxide, iodide/-iodate, cerium(III)/cerium(IV), ferroins/ferriins, and related complexes.

Cerium(III), chlorite ion, and the iron(II) terpyridine complexes are new ozone reductants investigated to form the basis for new residual ozone methods. They were selected because they possess higher standard reduction potentials than either iodide ion or arsenic(III) and therefore promise enhanced ozone selectivity. The iodate method and the cerium method promise ozone titer stability, whereas the iodate method, the cerium method, and the iron(II) terpyridine method promise great sensitivity.

BEGIN FIRST LINE OF TEXT HERE
CENTER OF PAGE
TOP OF IMAGE AREA
DROPPED HEAD: BEGIN SECTIONS HERE
9 1/8"
BEGIN LAST LINE OF TEXT
3/8"
BOTTOM OF IMAGE AREA. OUTSIDE DIMENSION FOR TABLES AND ILLUSTRATIONS
PAGE NUMBER
EPA Form 2350-4 (4-80)
(PREVIOUSLY CIN: EPA FORM 287)
TYPING GUIDE SHEET

BEGIN FIRST LINE OF TEXT HERE
CENTER OF PAGE
TOP OF IMAGE AREA
DROPPED HEAD: BEGIN SECTIONS HERE

SECTION 2

CONCLUSIONS AND RECOMMENDATIONS

1. Stability of the titer of the ozonated reagent solutions.

Convenient laboratory analysis demands stable ozonated reagent solutions. With the DPD method, the ozone titer changed so rapidly with time both for ozone in purified water and for ozone solutions with added hydrogen peroxide that the method cannot be recommended for routine ozone analysis. The arsenic(III) back titration titer steadily increased for ozone solutions with added hydrogen peroxide. The ozone titer by the amperometric method with excess sodium thiosulfate increased 4 percent in 9 minutes with ozone in purified water. The ozone titer determined by the arsenic(III) direct oxidation method and the Indigo method varied less than 3 percent over 3 hours even with added hydrogen peroxide.

2. Stability and calibration of the reagent solutions.

The arsenic(III) stock solutions used for the arsenic(III) direct oxidation method are stable standard solutions readily prepared by weight. Dilute working solutions should be prepared daily. Stock Indigo disulfonate would need replacement at least every four weeks. The Indigo trisulfonate stock solution is more stable and would require replacement only every ten weeks. Calibration of the Indigo dyes is essential, is time consuming, and is based on Iodometry. These problems could be avoided if higher purity dye were readily available and calibration could be based on weight.

3. Accuracy of the ozone titer.

The ozone titers differed among methods only when changes in the ozone-reductant reaction were involved. Conditions which reduce ozone decay prior to reaction with reductant reduced the scatter observed within a single method and reduced the differences observed among the analytical methods. All methods occassionally give a point 30-50 percent removed from that calculated on an otherwise smooth decay curve. This makes single point analysis for residual ozone untrustworthy.

The Indigo method minimizes ozone decay by operating at pH 2. Buffers which slow ozone decay increase the ozone concentration determined by direct arsenic(III) oxidation. Multiple analysis on tap water or acid stabilized ozone solutions show few differences.

BEGIN LAST LINE OF TEXT
3/8"
BOTTOM OF IMAGE AREA; OUTSIDE DIMENSION FOR TABLES AND ILLUSTRATIONS

EPA Form 2350-4 (4-80)
(PREVIOUSLY CIN. EPA FORM 287)
© U.S. GOVERNMENT PRINTING OFFICE 1981-665-008
TYPING GUIDE SHEET

4. UV method.

The direct measurement of the absorbance of aqueous ozone at 259 nm is the most straightforward and simplest ozone procedure. Here the absolute ozone concentration is based on the determination of the ozone absorption coefficient by comparison with an iodometric method. Significant differences exist in reported values for the absorption coefficient. In addition to this fundamental problem, the procedure suffers a practical problem. In waste water, many impurities absorb in the critical UV region and produce a large background absorption thus making the method applicable only to very pure solutions free from bacteria, turbidity and other absorbing materials.

5. Delta Electrode.

The Delta electrode failed to maintain calibration and failed to respond linearly over a 10 mg/L ozone range.

6. Alternative Reductants

All four exploratory methods failed to give reliable residual ozone values. The chlorite ion method failed because ozone does not selectively react with the excess chlorite ion to produce the measured chlorine dioxide; ozone also rapidly attacks the chlorine dioxide, thereby producing low ozone titers.

The stable iron(II) terpyridine complexes were oxidized by ozone to the unstable iron(III) state. Reaction conditions could not be found such that the iron(II) to iron(III) conversion quantitatively and consistently reflected ozone titers.

The cerium method failed because the cerium(IV) product seems to be readily reduced by wastewater impurities and ozone decay products. This resulted in significantly low ozone titers.

The failure of the iodate method was the most puzzling and troublesome. At low concentrations, iodine did not quantitatively disproportionate to iodate ion. Since valid ozone titers demand a 100% conversion of iodine to iodate ion, the iodate method failed.

7. Purging Technique

The purging technique is unreliable due to ozone decomposition during the purge and reabsorption steps.

8. Recommendation

No iodometric method is recommended. The Indigo method and the arsenic(III) direct oxidation method are the methods of choice (6). The Standard Methods committee should consider replacing the standard iodometric method currently in wide use with either the Indigo or the arsenic(III) direct oxidation method.

EPA Form 2350-4 (4-80)
(PREVIOUSLY CIN. EPA FORM 287)
PAGE NUMBER
TYPING GUIDE SHEET

SECTION 3

LITERATURE BACKGROUND

The oxidation of iodide ion to iodine by ozone with subsequent titration of the iodine formed is the classical method for the determination of residual ozone (2). Furthermore it is the reference method adopted by the EPA and it is the final calibration method for most other methods, (for example, indigo and the amperometric membrane electrode).

The reaction of ozone with iodide ion is described by

$$O_3 + I^- \rightarrow O_2 + IO^- \qquad \text{fast}$$

$$IO^- + H_2O \rightarrow HIO + OH^- \qquad \text{fast}$$

$$HIO + 2I^- \rightarrow I_3^- + OH^- \qquad \text{slow}$$

$$3\,HIO + 3OH^- \rightarrow IO_3^- + 2I^- + 3\,H_2O \qquad \text{very slow}$$

Upon acidification the species hypoiodite ion (IO^-), hypoiodous acid (HIO), and iodate ion (IO_3^-) are all converted to triiodide ion (I_3^-) so that the overall process is ideally

$$O_3 + 3I^- + H_2O \rightarrow I_3^- + O_2 + 2OH^-$$

and theoretically one molecule of ozone liberates one molecule of titratable triiodide ion, a complex of molecular iodine + iodide ion.

Thermodynamically, the ozone oxidation of iodide ion and iodine to form iodate ion is favored at high pH.

$$3O_3 + I^- \rightarrow 3O_2 + IO_3^-$$

$$5O_3 + I_2 + H_2O \rightarrow 5O_2 + 2IO_3^- + 2H^+$$

Furthermore, at a pH above 9, iodine is unstable, readily undergoing disproportionation

$$I_2 + 2OH^- \rightarrow IO^- + I^- + H_2O$$

$$3IO^- \rightarrow 2I + IO_3^-$$

EPA Form 2350-4 (4-80)
(PREVIOUSLY CIN, EPA FORM 2827)
TYPING GUIDE SHEET

Regardless of whether iodate ion is formed by direct oxidation or disproportionation of iodine, for every three moles of ozone absorbed, one mole of iodate ion should be formed.

In the standard iodometric method for analysis of ozone in water, ozone is purged into potassium iodide solution and after acidification with sulfuric acid the iodine is titrated with standard sodium thiosulfate (7). The ozone:iodine stoichiometry has been extensively studied and found to range from 0.65 to 1.5 (8-18). The factors affecting the stoichiometry include pH, buffer composition and concentration, iodide ion concentration, and sampling techniques. Modifications in the iodine determination include changes in end-point detection, pH, and back titration techniques.

Saltzman and Gilbert measured the rate of iodine formation following gas phase ozone addition to various iodide ion solutions and selected 1% potassium iodide in 0.1 M neutral phosphate buffer as the most satisfactory reagent because the maximum color, developed 45 minutes after sampling, represented an ozone:iodine stoichiometry of 1:1 (8). This unit stoichiometry was established by comparison with an independent method based upon conversion of the ozone to nitrogen dioxide by addition of excess nitric oxide. Assuming unit stoichiometry for 1% neutral phosphate buffered potassium iodide solution, Byers and Saltzman obtained a stoichiometry factor of 0.65 for 1% potassium iodide solutions at pH 14 (9).

Theoretically, the iodide ion reduction of ozone should liberate one molecule of oxygen in addition to the one molecule of iodine. Ingols, Feltner and Eberhardt measured both the iodine and oxygen formed on gas phase ozone addition to iodide ion solutions at pH 2 and 9 (10). They found twice as much iodine was liberated at pH 2 as at pH 9. At pH 9, one molecule of oxygen was liberated per molecule of iodine formed whereas at pH 2, very little oxygen was liberated. They also found more iodine was liberated at pH 7 than at pH 9. They concluded, therefore, that only at pH 9 was the ozone:iodine stoichiometry 1:1.

Boyd, Willis and Cyr determined an iodine:ozone stoichiometry of 1.53 ± 0.12 for 1% neutral phosphate buffered potassium iodide by comparison to independent gas phase spectrophotometric measurements of ozone (11). But this was challenged by Kopszynski and Bufalini who obtained an iodine:ozone ratio of 0.929 ± 0.32 by comparison to long path infrared analysis (12) and by Hodgeson, Baumgardner, Martin and Rehme who obtained an iodine:ozone ratio of 0.975 ± 0.067 using gas phase nitric oxide titration for the independent measurement of ozone concentration (13). Dietz, Pruzansky and Smith using a photometric ozone analyzer calibrated by the pressure change produced on the decomposition of ozone to oxygen confirmed that the iodine:ozone ratio increases with decreasing pH, although the magnitude of the effect is not very great, and that at nearly neutral pH, the stoichiometry is 1.00 ± 0.03 (14).

BEGIN FIRST LINE OF TEXT HERE
CENTER OF PAGE
TOP OF IMAGE AREA
DROPPED HEAD; BEGIN SECTIONS HERE
BEGIN LAST LINE OF TEXT
3/8"
BOTTOM OF IMAGE AREA; OUTSIDE DIMENSION FOR TABLES AND ILLUSTRATIONS
EPA Form 2350-4 (4-80)
(PREVIOUSLY CIN, EPA FORM 287)
PAGE NUMBER
TYPING GUIDE SHEET

Flamm found that the use of 1% potassium iodide in boric acid buffer gave gas phase ozone titers consistently in agreement with UV spectrophotometry for 0.35 to 3.5 mg/L ozone whereas 1% potassium iodide in neutral phosphate buffer gave ozone titers that steadily increased with time and that were 15-30% high (15). This error was attributed to the formation of a second product in addition to iodine. The second product, tentatively identified as hydrogen peroxide, reacts with iodide ion to form iodine.

Parry and Hern suggest that iodate ion formation could be partially responsible for the present discord since the oxidation of iodide ion to iodate ion 1) is significant at high ozone concentrations, 2) is sensitive to catalysts such as a borosilicate glass frit, 3) is favored by increasing pH, and 4) is important not only in alkaline solutions but in neutral solutions as well (16).

Bergshoeff, Lanting, Prop and Reynders described an absorbing solution for gas phase ozone which was 1% potassium iodide, 2% potassium bromide in 0.02 M neutral phosphate buffer and contained a known amount of sodium thiosulfate (17). The potassium bromide and lower buffer concentration eliminated the influence of sampling flow rate and relative humidity on stoichiometry. The sodium thiosulfate stabilized the sample so that the ozone titer remainded unchanged for at least two days. An iodine:ozone stoichiometry of 0.96 ± 0.02 was calculated using gas phase titration with excess nitric oxide for the independent ozone measurement.

Sullivan, Hall, D'Ambrosi and Roth added aqueous ozone to 2% potassium iodide in 0.1 M neutral phosphate buffer containing a known amount of arsenic(III) and back titrated the excess arsenic(III) with iodine to a starch endpoint (18). This Arsenic(III) Back Titration method was compared with Flamm's 1% potassium iodide boric acid method and with the Standard Iodometric Method. The liberated iodine was titrated with sodium thiosulfate without changing from pH 5 for Flamm's method and after acidification with sulfuric acid for the Standard Iodometric Method. The Arsenic(III) Back Titration method gave average ozone concentrations that were 7% to 20% lower than the other two methods.

Two standard methods for residual chlorine analyses, the amperometric method and the Palin DPD method, have been adapted for residual ozone analyses (7,19). In the amperometric method, ozone oxidizes iodide ion in acetate buffer of pH 4.0 - 4.5 in the presence of a known excess of sodium thiosulfate, phenylarsine oxide (PAO) or inorganic arsenic(III). Without acidification, these excess reagents are then titrated with standard iodine to an amperometric endpoint. In the DPD method, ozone oxidizes iodide ion in phosphate buffer of pH 6.4. The liberated iodine then oxidizes N,N-diethyl-p-phenylenediamine cation (DPD) to a pink Wurster cation which is quantitated colorimetrically or is titrated with standard ferrous ammonium sulfate. If iodide ion is omitted from the phosphate buffer solution, very little color develops because ozone oxidizes DPD to the colorless quinone diimine cation (Fig. 1).

BEGIN FIRST LINE OF TEXT HERE
CENTER OF PAGE
TOP OF IMAGE AREA
DROPPED HEAD, BEGIN SECTIONS HERE
BEGIN LAST LINE OF TEXT
3/8"
BOTTOM OF IMAGE AREA; OUTSIDE DIMENSION FOR TABLES AND ILLUSTRATIONS
PAGE NUMBER
EPA Form 2350-4 (4-80)
(PREVIOUSLY CIN, EPA FORM 287)
TYPING GUIDE SHEET

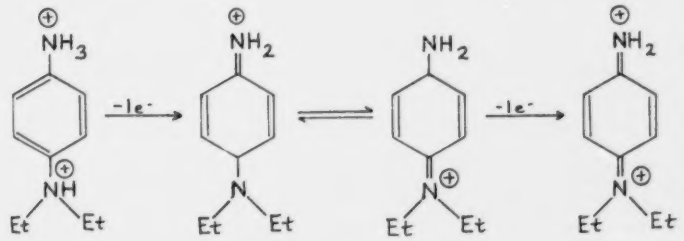

DPD diamine cation colorless | Wurster cation pink | quinone diimine cation colorless

Figure 1. The DPD Method

In the iodometric methods, theoretically both the pH during the initial ozone:iodide reaction and the pH during the iodine determination can alter the ozone:iodine stoichiometry. The ozone:iodine ratio could decrease with decreasing pH due to

$$4O_3 + 10\ HI \rightarrow 5I_2 + H_2O_2 + 4H_2O + 3O_2$$

Hydrogen peroxide could oxidize iodide ion leading to excess iodine

$$H_2O_2 + 2I^- + 2H^+ \rightarrow I_2 + 2H_2O$$

Air oxidation of iodide ion in acid leads to a decrease in O_3:I_2 ratio

$$O_2 + 4I^- + 4H^+ \rightarrow 2I_2 + 2H_2O$$

Therefore, as the pH decreases for the ozone oxidation of iodide ion, the quantity of iodine should increase due to less iodate ion formation, hydrogen peroxide formation, and air oxidation of iodide ion. As the pH for the iodine determination decreases, the iodine titer should increase due to reconversion of iodate ion to iodine and air oxidation of iodide ion.

This work examines and compares the four currently popular iodometric methods for aqueous ozone analysis listed in Table 1. The importance of iodate ion and hydrogen peroxide (which can arise from the auto-decomposition of ozone itself) is investigated and the pH and buffer effects on ozone analyses are analyzed. These analytical methods are also compared with the four non-iodometric methods for ozone analysis described in Table 2.

BEGIN FIRST LINE OF TEXT HERE
CENTER OF PAGE
TOP OF IMAGE AREA
DROPPED HEAD, BEGIN SECTIONS HERE
BEGIN LAST LINE OF TEXT
BOTTOM OF IMAGE AREA; OUTSIDE DIMENSION FOR TABLES AND ILLUSTRATIONS
3/8"
PAGE NUMBER
EPA Form 2350-4 (4-80)
(PREVIOUSLY CIN. EPA FORM 287)
TYPING GUIDE SHEET

TABLE 1. IODOMETRIC METHODS FOR OZONE ANALYSIS

Method	O_3 Reduction Excess reagent	pH	I_2 titration pH
Iodometric	none	3.5-9.0	2
Amperometric	$S_2O_3^=$	4.5	4.2-6.8
	PAO or As(III)		
As(III) Back	As(III)	6.8	6.8
DPD	DPD	6.4	6.4

TABLE 2. NON-IODOMETRIC METHODS FOR OZONE ANALYSIS

Method	Reductant	pH
Indigo	C=C	2.0
As(III) Direct	As(III),PAO	6.5-7.0
Delta electrode	e^-	
UV	none	

The indigo method is performed at pH 2 (4). Ozone adds across the carbon-carbon double bond of sulfonated indigo dye and decolorizes it. The change in absorbance is determined spectrophotometrically. In the direct oxidation of As(III), ozone reacts with either inorganic As(III) or PAO at pH 4-7, the pH is adjusted to 6.5-7 and the excess As(III) species is back titrated with standard iodine to a starch endpoint (3).

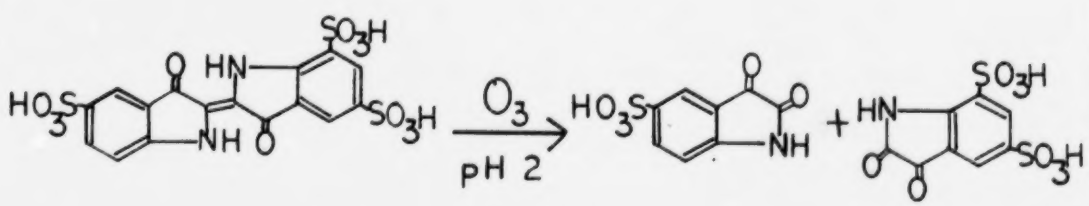

blue colorless

The Delta electrode operates at a high potential and selectively reduces the molecular ozone transported to the cathode through a teflon membrane (5). It measures ozone in situ and can be used as a continuous monitor. The UV method measures the absorbance of aqueous ozone at 259 nm and is applicable only to very pure solutions free from turbidity and other materials that absorb in the critical UV region (4). The last two methods involve no reagents and no pH specifications.

The methods in Table 2 are technically non-iodometric methods because ozone is measured by its interaction with something other than iodide ion. However, not one of these methods is totally independent of iodometry. The indigo reagent and the Delta electrode both require calibration against a standard ozone solution whose concentration has been determined by an iodometric method or by direct measurement of the UV absorbance of ozone at 259 nm. The direct UV measurement is based on a molar absorptivity determined by an iodometric method. Therefore, all concentrations of ozone are finally based on the iodometric method and any error in the iodometric method is carried into the indigo method, the Delta electrode, and the direct UV method.

The direct UV method is based on a molar absorptivity of 2900 M^{-1} cm^{-1} at 258 nm. This was determined both by Kilpatrick and Herrick in 1965 (20) and by Bader and Hoigné in 1976 (21) by iodometric methods. Recently, Hart has published a molar absorptivity of 3300 M^{-1} cm^{-1} at 260 nm (22,23). These values for the molar absorptivity of ozone at 258-260 nm differ by 14 percent. Therefore, the absolute calibration of these non-iodometric methods could be in error by 14 percent.

The arsenic(III) direct oxidation method is the least dependent on iodometry because arsenic(III), the reductant for ozone, is a primary standard. The excess arsenic(III) remaining after ozone addition is back titrated with standard iodine, but the complication of air oxidation inherent in the iodide ion/iodine reactions is minimized since iodide ion is introduced only with the standard triiodide ion solution and since the titration is performed at neutral pH.

In the pH range 6-9 which brackets typical waste water acidity, ozone has a half-life ranging from 14 minutes to 2 minutes respectively. Under these conditions, ozone concentrations vary significantly over the sampling time required to make comparisons by the usual repetitive sample method. A kinetic technique was developed for producing ozone solutions of known concentration in the 24-0 mg/L range (24). A steady state solution of ozone is prepared and then allowed to decompose. At known time intervals during the decomposition process, the ozone level of the solution is determined by two or more different analytical methods. The resulting time-concentration profile for each analytical method is graphed and is fitted to the generalized rate law using FIT 80. FIT 80* is a computer program based on the method of

$$\frac{-d[O_3]}{dt} = k_1[O_3][OH^-] + k_2[O_3]^2$$

Gauss which allows the simultaneous least squares fitting of first and second order parallel reactions.

*See McWilliams, P., et al., Rev. Sci., & Inst., 33:70, 1965.

BEGIN FIRST LINE OF TEXT HERE
CENTER OF PAGE
TOP OF IMAGE AREA
DROPPED HEAD, BEGIN SECTIONS HERE
BEGIN LAST LINE OF TEXT
3/8"
BOTTOM OF IMAGE AREA; OUTSIDE DIMENSION FOR TABLES AND ILLUSTRATIONS
PAGE NUMBER
EPA Form 2350-4 (4-80)
(PREVIOUSLY CIN, EPA FORM 287)
© U.S. GOVERNMENT PRINTING OFFICE 1981-560-650
TYPING GUIDE SHEET

The kinetic and mechanistic description of the decomposition of aqueous ozone has been extensively investigated but no detailed mechanism is generally accepted. Results indicate that decay leads to free radicals. The half-life of dissolved ozone is readily affected by pH, UV light, concentration of ozone and concentration of radical scavengers (21,25,26). The experimental results published prior to and during the 1950's fit either a one-term or a two-term rate law (25). Recent works of Hoigné (26) and Hart (22,23) also support a two-term rate law. This rate law is a mathematical model which describes time-concentration curves for ozone decay and does not relate directly to a specific mechanism. The calculated rate constants are apparent rate constants and not true rate constants. They are calculated and compared for each kinetic run and are used for method comparisons within each run and not between different runs. The kinetic parameters calculated for each method should be identical if each method gives the same result.

Even though a mechanism is not necessary for the application of the kinetic technique since comparisons among calculated kinetic parameters indicate discrepancies among methods, a general mechanistic scheme aids understanding of potential method differences.

Based on a set of clever experiments, Hoigné (26) has recently proposed the mechanism shown below:

$$O_3 + OH^- \rightarrow O_2^{\bullet -} + HO_2^{\bullet} \qquad k_{OH^-} \sim 170\ M^{-1}sec^{-1}$$

$$O_2^{\bullet -} + O_3 \xrightarrow{+H^+} OH^{\bullet} + 2\ O_2 \qquad k_{O_2^{\bullet -}} \sim 1.6 \times 10^9\ M^{-1}sec^{-1}$$

$$OH^{\bullet} + \text{scavenger} \rightarrow \text{products}$$

$$OH^{\bullet} + O_3 \xrightarrow{-H^+} O_2 + O_2^{\bullet -} \qquad k_{OH^{\bullet}} \sim 4.7 \times 10^8\ M^{-1}sec^{-1}$$

$$O_2^{\bullet -} + O_3 \rightarrow OH^{\bullet} + 2O_2$$

$$2\ HO_2^{\bullet} \rightarrow H_2O_2 + O_2$$

$$HO_2^{\bullet} + O_2^{\bullet -} \rightarrow HO_2^- + O_2$$

$$H_2O_2 + OH^- \rightarrow H_2O + HO_2^- \qquad pK_a = 11.65$$

$$HO_2^- + O_3 \rightarrow OH^{\bullet} + 2O_2 \qquad k_{HO_2^-} \sim 5 \times 10^6\ M^{-1}sec^{-1}$$

BEGIN FIRST LINE OF TEXT HERE
CENTER OF PAGE
TOP OF IMAGE AREA
DROPPED HEAD; BEGIN SECTIONS HERE
BEGIN LAST LINE OF TEXT
3/8"
BOTTOM OF IMAGE AREA OUTSIDE DIMENSION FOR TABLES AND ILLUSTRATIONS
PAGE NUMBER
EPA Form 2350-4 (4-80)
(PREVIOUSLY CIN: EPA FORM 267)
TYPING GUIDE SHEET

Ozone decay is initiated by hydroxide ion attack on ozone to form the superoxide radical anion ($O_2^{\bullet -}$) and the hydroperoxyl radical ($HO_2^{\bullet}$). Then in a diffusion controlled reaction, superoxide radical anion reacts with a second ozone molecule to form the hydroxyl radical ($OH^{\bullet}$). This hydroxyl radical can either react with any radical scavenger present or can react with an ozone molecule in a diffusion controlled reaction to generate another superoxide radical anion which in turn reacts with ozone to generate another hydroxyl radical.

The hydroperoxyl radical, a by-product of ozone decay, can dimerize to hydrogen peroxide or can react with the superoxide radical anion to form the hydroperoxyl anion. Hydrogen peroxide reacts with ozone slowly. Hydroperoxyl anion, however, can catalyze ozone decay by attack on ozone to form the hydroxyl radical in a very fast reaction. A hydrogen peroxide concentration in excess of 3.2 μg/L will make the reaction of hydroperoxyl anion with ozone as important as the reaction of hydroxide ion with ozone. The concentration of hydrogen peroxide found as a reaction product increases with a decrease in pH.

According to this mechanism, the lifetime of ozone in aqueous solution depends on added solutes or impurities. The hydroxyl radical, which forms upon ozone decomposition, is a chain carrier for further ozone decomposition and any solute or impurity which scavenges this radical will retard ozone decomposition.

Hart (22,23) has also recently proposed the following chain process for the hydroxide ion initiated decomposition of aqueous ozone. The mechanism is based on the spectroscopic observation of ozonide radical anions, $O_3^{\bullet -}$, and superoxide radical anions, $O_2^{\bullet -}$, and on the chemical reactions of the hydroxyl radical.

$$O_3 + OH^- \rightarrow O_3^{\bullet -} + OH^{\bullet}$$

$$O_3 + OH^- \rightarrow HO_2^- + O_2$$

$$HO_2^- + O_3 \rightarrow HO_2^{\bullet} + O_3^{\bullet -}$$

$$O_3^{\bullet -} \rightleftharpoons O^{\bullet -} + O_2$$

$$O^{\bullet -} + H_2O \rightleftharpoons OH^{\bullet} + OH^-$$

$$HO_2^{\bullet} \rightleftharpoons H^+ + O_2^{\bullet -}$$

$$O_2^{\bullet -} + O_3 \rightarrow O_3^{\bullet -} + O_2$$

EPA Form 2350-4 (4-80)
(PREVIOUSLY CIN. EPA FORM 287)
TYPING GUIDE SHEET

Ozone decay is initiated by hydroxide ion attack on ozone to form the hydroperoxyl anion, and/or the ozonide radical anion plus the hydroxide radical anion. The hydroperoxyl anion reacts with a second ozone molecule to form the hydroperoxyl radical and the ozonide radical anion. The ozonide radical anion produces hydroxyl radicals on dissociation through O.-. The hydroperoxyl radical dissociates to the superoxide radical anion which reacts with another ozone molecule to form the ozonide radical anion. The hydroxyl radical functions as a chain carrier and any species which scavenges this radical retards ozone decomposition.

The build up of the superoxide radical anion under the favorable conditions of high pH and high hydrogen peroxide concentrations could complicate the analysis of ozone by the UV method because this long lived species absorbs at 260 nm. A simplified mechanism consistent with Hoigne's model and Hart's model is shown below.

$$O_3 + OH^- \underset{k_b}{\overset{k_a}{\rightleftharpoons}} [O_3 \cdot OH^-]$$

$$[O_3 \cdot OH^-] \xrightarrow{k_c} O_3 \cdot^-,\ HO_2 \cdot,\ OH \cdot,\ H_2O_2 + \text{products}$$

$$[O_3 \cdot OH^-] + O_3 \xrightarrow{k_d} \text{products}$$

Initially ozone complexes with hydroxide ion and this reactive intermediate can undergo either a first order electron transfer reaction or a second order reaction with ozone. The first order electron transfer reaction could lead to the formation the superoxide radical anion, the hydroperoxyl radical and the hydroxyl radical which in turn either act as chain propagators and lead to further ozone decay or react with radical scavengers to form other products. The second order reaction of ozone with the ozone-hydroxide intermediate leads directly to products without formation of discrete short-lived radical intermediates.

This simple model is consistent with the two term rate law for parallel first and second order reactions used by FIT 80 to describe the time-concentration curves for the kinetic technique.

EPA Form 2350-4 (4-80)
(PREVIOUSLY CIN, EPA FORM 287)
TYPING GUIDE SHEET

SECTION 4

EXPERIMENTAL PROCEDURES

Water. Purified water was prepared by passing distilled water through a charcoal column, two mixed bed deionization columns, and a filtering column of a Barnstead Nanopure Water Purification system. The water leaving this system had a conductivity of 18.3 megaohm-cm. This water was then distilled in a Barnstead bi-distiller all glass still and was stored in polyethylene or glass bottles. This water is termed "purified water".

Reagents. All chemicals were of ACS reagent grade. All solutions were prepared in purified water by standard methods.

Ozone. Ozone was generated from dry oxygen by an Ozone Research and Equipment Corporation (OREC, Phoenix, AZ) Model 03V9-0 ozonator. Ozone solutions were prepared in a 3000 ml contactor equipped with a medium porosity glass frit and a sampling stopcock with a Luer tip. Additional stopcocks allowed the inclusion of a closed flow loop for mixing and for the Delta electrode. A Cole-Parmer (Chicago, IL) Model 7149-10 all telfon pump provided circulation (Fig. 2).

When using purified water, the steady state ozone concentration in the contactor generally was 22 mg/L. Lower steady state concentrations were achieved by bubbling the ozonated oxygen first through a 2000 ml tower containing sodium hydroxide solutions. Sodium hydroxide solutions of pH 10.3, 11.4, and 12.5 in the tower produced steady state ozone levels in the contactor of 7-8 mg/L, 5-6 mg/L, and 3-5 mg/L, respectively.

A water jacketed 500 ml contactor was used to compare rate constants between runs. (Fig. 3). A Forma Scientific (Marietta, OH) Model 2095-2 water bath circulated coolant to the water jacket. During ozonation a medium porosity glass frit was suspended in the contactor. After ozonation the frit was removed and a tightly-fitting teflon plunger was placed in contact with the upper surface of the aqueous solution. In this manner, the entire contactor became "shrinking bottle". The sampling stopcock with Luer tip was located on the bottom to maximize available solution. Only glass or teflon came in contact with aqueous and gaseous ozone in all towers, contactors, and tubing.

BEGIN FIRST LINE OF TEXT HERE
CENTER OF PAGE
TOP OF IMAGE AREA
DROPPED HEAD: BEGIN SECTIONS HERE
9-1/8"
BEGIN LAST LINE OF TEXT
3/8"
BOTTOM OF IMAGE AREA; OUTSIDE DIMENSION FOR TABLES AND ILLUSTRATIONS
PAGE NUMBER
EPA Form 2350-4 (4-80)
(PREVIOUSLY CIN. EPA FORM 287)
TYPING GUIDE SHEET

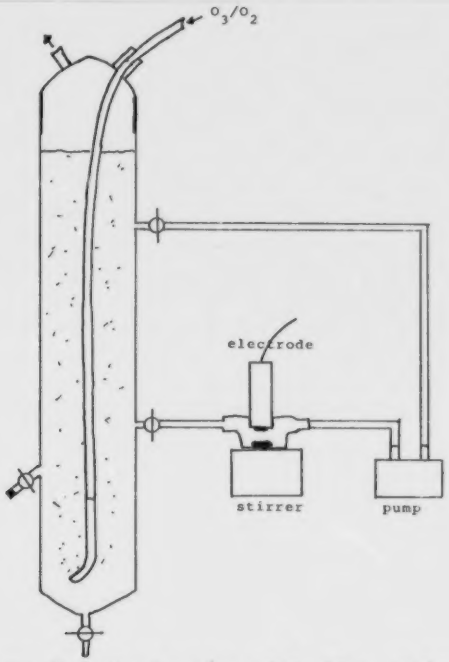

Figure 2. Contactor with Flow Cell.

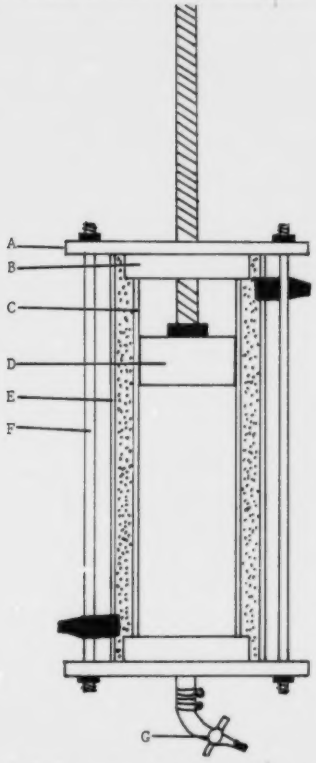

A. Aluminum Sheet
B. Teflon
C. Precision Bore Glass Tubing
D. Teflon Plunger
E. Plexiglass Water Jacket
F. Brass Rod
G. Stopcock with Luer Tip

Figure 3. Water Jacketed Contactor.

EPA Form 2350-4 (4-80)
(PREVIOUSLY CIN. EPA FORM 287)
TYPING GUIDE SHEET

Sampling. Briefly open the sampling stopcock to fill with fresh solution. Fit a Silverman Syringe, calibrated by weight, to the Luer joint of the stopcock. Open the stopcock and allow the syringe to gravity fill. Fit the syringe with a flexible tip made of heat shrinkable polyethylene, remove gas bubbles, bring the syringe to volume and inject the ozone solution below the surface of the solution containing the reductant.

The Silverman syringe was either a multi-stop model (Fig. 4) or a one stop model (Fig. 5). The multi-stop model was designed to minimize sampling time in the multiple analyses for kinetic runs.

Glassware. Prior to initial use, all glassware and teflon stir bars were washed in an Alconox solution in distilled water. After a thorough distilled water rinse, each piece was soaked in 1:1 nitric acid for a minimum of 1 hour, thoroughly rinsed with distilled water, and finally rinsed with purified water.

Each piece of glassware was then exclusively used for one procedure. Cleaning between successive uses was limited to the Alconox wash and distilled water rinse. This repetitive use for the same procedure was used to maximize reproducibility.

Instrumentation

UV-Vis Spectrophotometry. All ultraviolet-visible absorption measurements were made on a Hewlett Packard 8450A UV-Vis spectrophotometer which was equipped with thermostated cell holders and holders for cells of 1-10 cm path length. Generally for a methods comparison, the non-thermostated 1 cm cell holders were used and the contactor was sampled for each UV point. The thermostated cell holders were used to follow ozone decomposition in the cell itself without resampling from the contactor for each point.

pH. The pH was measured either on a Radiometer (Copenhagen, Denmark) PHM 64 digital pH meter or a Radiometer PHM 26 pH meter.

Differential Pulse Polarography. A Princeton Applied Research Corporation (PAR, Princeton, NJ) Model 174 A polarographic analyzer, Model 174/50 drop timer and a Hewlett Packard (Avondale, PA) Model 7040 X-Y recorder were used for all differential pulse polarographic (DPP) measurements.

Autotitration System. A Metrohm Herisau (Brinkman Instruments, Westbury, NY) Model E535 or Model E415 dosimat delivered the titrant. Various 5 ml, 10 ml and 20 ml burets were used. The amperometric endpoint was detected using two platinum foils (~2 cm^2) placed about 0.5 cm apart. The voltage source was a Metrohm Herisau Model E585 polarizer. The polarization voltage was set at 50 mV. The current-volume relationship was monitored and recorded on a Metrohm Herisau Model E536 potentiograph.

BEGIN FIRST LINE OF TEXT HERE
CENTER OF PAGE
TOP OF IMAGE AREA
DROPPED HEAD, BEGIN SECTIONS HERE
9-1/8"
BEGIN LAST LINE OF TEXT
3/8"
BOTTOM OF IMAGE AREA, OUTSIDE DIMENSION FOR TABLES AND ILLUSTRATIONS
PAGE NUMBER
EPA Form 2350-4 (4-80)
(PREVIOUSLY CIN, EPA FORM 287)
TYPING GUIDE SHEET

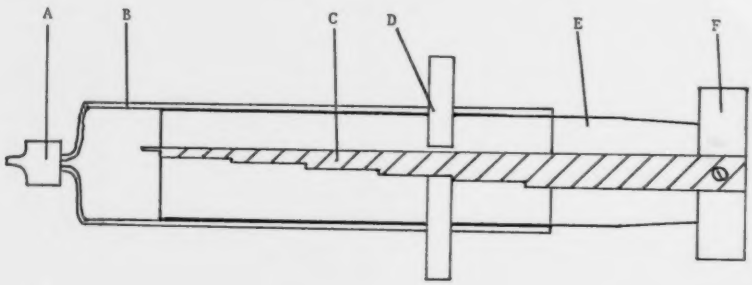

A. Teflon Adaptor
B. 50 ml Syringe Barrel
C. "Five-step" Brass Rod
D. Plexiglass Cuide
E. Syringe Plunger
F. Brass Cap

Figure 4. Multi-Stop Calibrated Syringe.

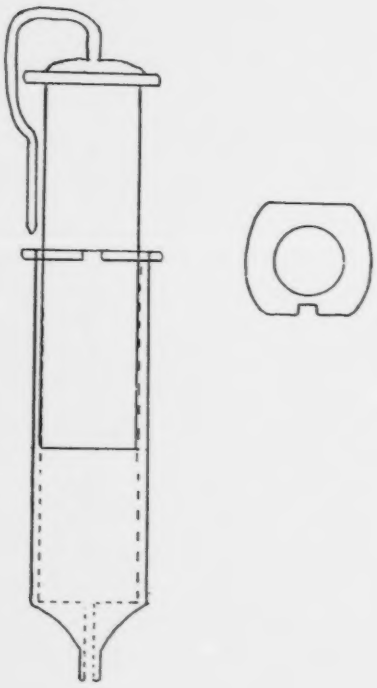

Figure 5. One Stop Calibrated Syringe.

DPD Method. The published procedure (19) was altered three ways in this work. Firstly, the DPD Indicator was increased from 5 ml to 10 ml in order to make color formation independent of DPD concentration for the ozone/iodine concentration range of interest. Secondly, the absorbance was measured at 552 nm to gain increased sensitivity (Fig. 6). Thirdly, calibration was based on iodine. The recommended potassium permanganate calibration gave good straight line plots of absorbance vs. [$KMnO_4$]. But, when the normality of an iodine solution standardized against As(III) was compared with normality determined by the DPD method calibrated with potassium permanganate, the ratio N(As(III)/N(DPD) was 1.15. No iodide ion is present in the published potassium permanganate calibration. When iodide ion was included in a potassium permanganate calibration the calibration curve was altered and the comparison of iodine normality based as As(III) with the iodine normality based on DPD, yielded N(As(III)/N(DPD) = 0.74. Ozone analyses are based on the iodine-DPD reaction and calibration should be based on standard iodine.

The absorbance at 552 nm varies significantly with the time lapse between ozone addition and measurement of absorbance. Hydrogen peroxide increases the rate of absorbance change. (Fig. 7). In this work the absorbance was read within 1-2 minutes of ozone addition to minimize this large source of error on the ozone titer.

Arsenic(III) Back Titration Method. The published procedure (18) was used but with agitation during ozone addition with a teflon coated magnetic stir bar. The time interval between ozone sampling and iodine back titration did not alter the ozone titer. With added hydrogen peroxide, the ozone titer steadily increased with time. (Fig. 8).

Indigo Method. Initial standard ozone solutions needed for construction of calibration curves were prepared as published (4) by bubbling ozonated oxygen through a medium porosity glass frit into purified water acidified to pH 2 with 1 M phosphoric acid and chilled to 2°-5°C with an ice/salt bath. The steady state concentration of ozone in this stock solution was generally 40 mg/L as determined by direct measurement of the UV absorbance at 259 nm. A lower concentration, typically 15 mg/L, needed for construction of the calibration curve was obtained by dilution with water acidified and chilled as above. Fogging of the UV cell during measurements on these cold solutions was troublesome. Sampling was done with Silverman calibrated syringe but the syringe had to be suction filled. To avoid these two problems, the following procedure for the preparation of standard ozone solutions was adopted.

Fill the contactor with purified water acidified to pH 2 with phosphoric acid and equilibrated to room temperature (20-23°C). Bubble ozonated oxygen through the solution for 15 min. Measure the ozone concentration by the direct UV method on four individual samples, inject four or five aliquots into prepared indigo volumetrics, and then remeasure the ozone concentration by the direct UV method on four individual samples. Remove an aliquot of the ozone solution and replace it with an equal volume of 20-23°C purified water acidified as above. Mix the solution with the teflon pump, redetermine the ozone concentration and sample the indigo volumetrics as above.

BEGIN FIRST LINE OF TEXT HERE
CENTER OF PAGE
TOP OF IMAGE AREA
DROPPED HEAD BEGIN SECTIONS HERE
BEGIN LAST LINE OF TEXT
3/8"
BOTTOM OF IMAGE AREA OUTSIDE DIMENSION FOR TABLES AND ILLUSTRATIONS
PAGE NUMBER
EPA Form 2350-4 (4-80)
(PREVIOUSLY CIN. EPA FORM 287)
TYPING GUIDE SHEET

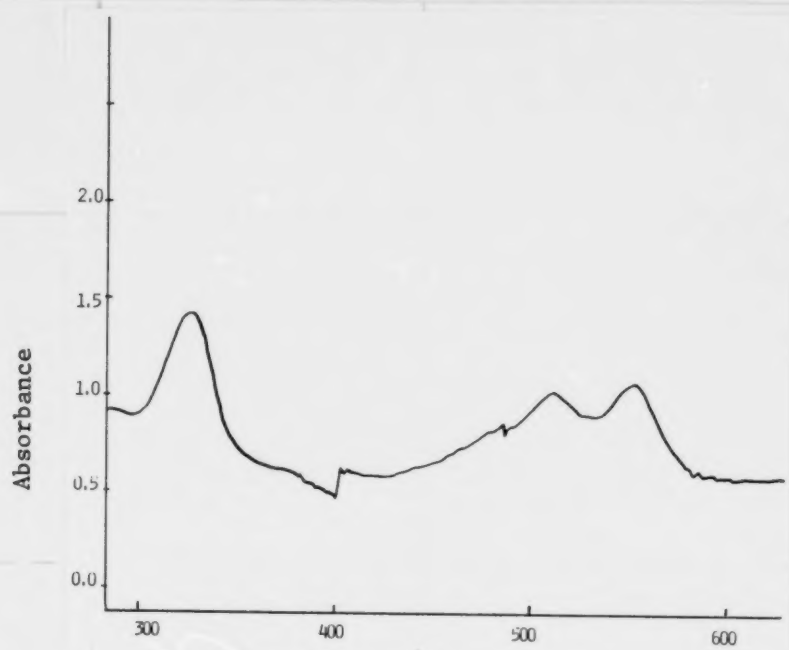

Figure 6. UV Visible Spectrum of DPD.

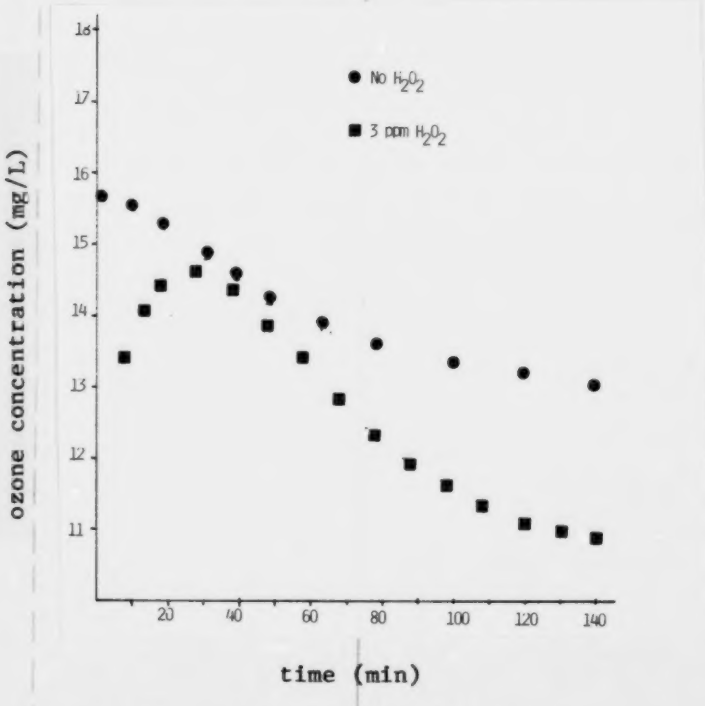

Figure 7. Stability of Ozone Titer for DPD.

Typically the time lapse between the first and the final UV measurement on a given concentration was 10 min. Over this time interval, the ozone concentration was stable with 3% (Table 3). Four or five different ozone concentrations were used to define the calibration curve.

TABLE 3. STABILITY OF OZONE IN WATER AT PH 2

mg/L O_3	S.D.	% R.E.
22.35	0.25	1.12
15.65	0.26	1.66
10.62	0.08	0.75
7.76	0.18	2.32
5.56	0.11	1.98
3.97	0.12	3.02

The calibration of freshly prepared stock solutions of sodium indigo disulfonate (Fisher) and potassium indigo trisulfonate (Aldrich supplied by Riedel-deHaen AG) gave reproducible slopes. Two examples are shown below:

disulfonate Batch 1	Abs = 1.28 - 0.42 $[O_3]$
disulfonate Batch 2	Abs = 1.27 - 0.44 $[O_3]$
trisulfonate Batch 1	Abs = 0.84 - 0.41 $[O_3]$
trisulfonate Batch 2	Abs = 1.15 - 0.42 $[O_3]$

All indigo stock solutions faded with time. In 7 weeks, the disulfonate Batch 1 faded to 53% of its original absorbance at 610 nm and its calibration curve was described by the equation Abs = 0.68 - 0.35 $[O_3]$. The different intercepts are readily corrected by an appropriate blank, but the different slopes lead to low ozone values particularly at high ozone concentrations. At the end of 14 weeks, the absorbance of the disulfonate Batch 1 was only 7% of its original value (93% loss). Table 4 shows the weekly change for Disulfonate Batch 4. Indigo trisulfonate stock solutions were significantly more stable. After 7 weeks trisulfonate Batch 1 maintained 91.6% original absorbance (Table 5).

BEGIN FIRST LINE OF TEXT HERE
CENTER OF PAGE
TOP OF IMAGE AREA
DROPPED HEAD BEGIN SECTIONS HERE
BEGIN LAST LINE OF TEXT
3/8"
BOTTOM OF IMAGE AREA, OUTSIDE DIMENSION FOR TABLES AND ILLUSTRATIONS
EPA Form 2350-4 (4-80)
(PREVIOUSLY CIN, EPA FORM 287)
PAGE NUMBER
U.S. GOVERNMENT PRINTING OFFICE: 1981 0-341-334
TYPING GUIDE SHEET

TABLE 4. DECOMPOSITION OF INDIGO DISULFONATE STOCK SOLUTIONS

BATCH - 4

Week	Abs. 610 nm	% original
0	0.7917	
1	0.7971	101
2	0.7622	96
3	0.7116	90
4	0.6545	83
5	0.6028	76
7	0.4805	61

TABLE 5. DECOMPOSITION OF INDIGO TRISULFONATE STOCK SOLUTIONS

BATCH 1

Week	Abs. 600 nm	% Original
0	0.8575	
1	0.8431	98.3
2	0.8348	97.4
4	0.8220	95.9
7	0.7857	91.6
10	0.7046	82.2

The absorbance of an ozonated indigo solution is stable. The ozone titer calculated from the absorbance varies less than 2.5% over 3 hours even in the presence of added hydrogen peroxide. (Fig. 9).

REGIN FIRST LINE OF TEXT HERE
CENTER OF PAGE
TOP OF IMAGE AREA
DROPPED HEAD, BEGIN SECTIONS HERE
6-1/2"
3/8"
BEGIN LAST LINE OF TEXT
BOTTOM OF IMAGE AREA, OUTSIDE DIMENSION FOR TABLES AND ILLUSTRATIONS
PAGE NUMBER
EPA Form 2350-4 (4-80)
(PREVIOUSLY CIN. EPA FORM 267)
TYPING GUIDE SHEET

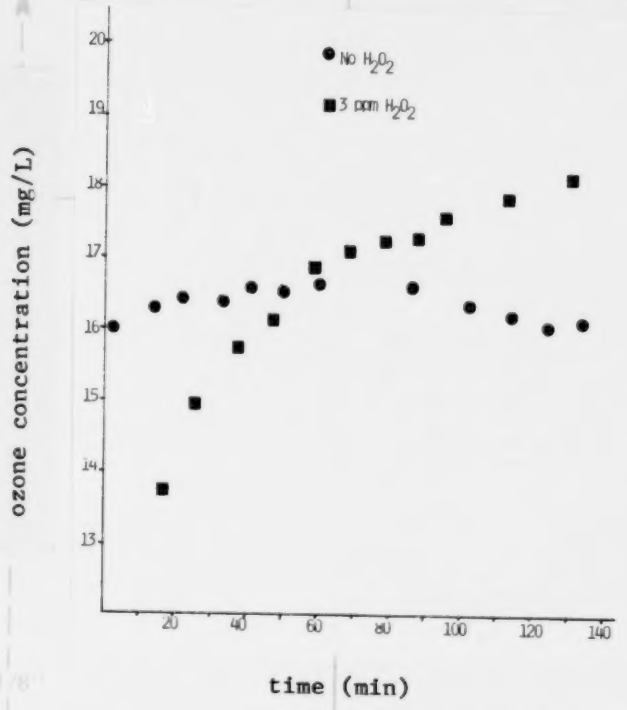

Figure 8. Stability of Ozone Titer for As(III) Back Titration.

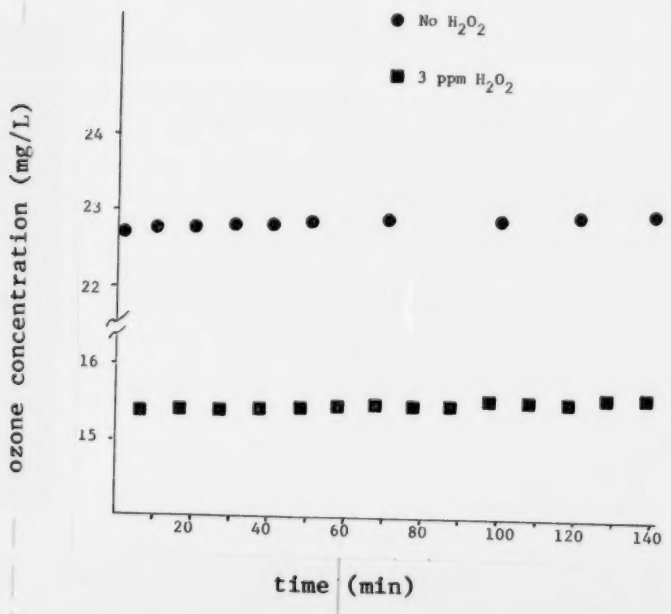

Figure 9. Stability of Ozone Titer for Indigo.

Arsenic(III) Direct Oxidation Method

Analytical Procedure, Phosphate Buffer. To a 125 ml Erlenmeyer flask, add a teflon coated magnetic stir bar, 25 ml 0.1 M neutral phosphate buffer, and a precisely measured 10.00 ml aliquot of 0.001 N arsenic(III) oxide solution. With stirring, add 10.00 ml ozone sample to the flask. Add Thyodene starch indicator and titrate the excess arsenic(III) oxide with standard 0.001 N iodine solution to a pale blue end-point. The 10.00 ml aliquot of 0.001 N arsenic(III) oxide solution will measure the residual ozone in a 10.00 ml sample containing up to 24 mg/L. A 5.00 ml As(III) aliquot and a 15.00 ml As(III) aliquot will measure up to 12 mg/L and 36 mg/L residual ozone respectively.

The time interval between the ozone sampling and the iodine titration of excess arsenic(III) did not alter the ozone titer. (Fig. 10).

Analytical Procedure, Acetate Buffer. Mix 41.5 ml 2 M sodium acetate and 415.0 ml 2 M acetic acid and dilute to one liter. Put 2 ml acetate buffer, 25 ml purified water, 10.00 ml .001 N arsenic(III) oxide solution, and a teflon coated magnetic stir bar in a 125 ml Erlenmeyer flask. With stirring add 10.00 ml ozone sample to the flask. Add 10 ml neutral phosphate buffer and titrate the excess arsenic(III) oxide with standard 0.001 N iodine solution to a pale blue Thyodene end-point.

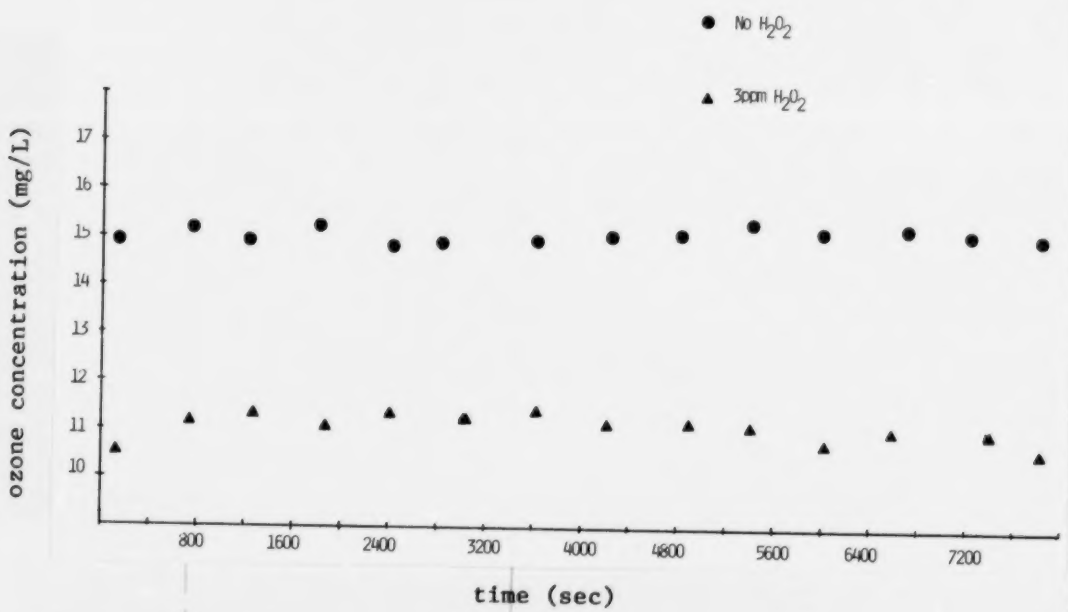

Figure 10. Stability of Ozone Titer for As(III) Direct Oxidation.

The Chlorite Ion Method

Reactions between Chlorite Ion and Ozone. Sodium chlorite (Kodak) solutions in 8×10^{-4} M sodium hydroxide were prepared by weight from the vacuum dried salt. The ozone measurements using chlorite ion were conducted in 2.00 cm cylindrical spectrophotometer cells that were fitted with a ground glass stopper. Typically the cells contained 1.739 ml of 7.26×10^{-2} M chlorite ion solution, 2.586 ml of 1×10^{-3} M acetate buffer, and a small teflon coated magnetic stir bar.** A 1.041 ml aliquot of ozone solution was injected into the rapidly stirring chlorite ion solution. The cell was quickly stoppered and the absorbance at 358.5 nm was measured against a reference cell which contained 2.586 ml of acetate buffer and 2.780 ml water.

Chlorine dioxide has a molar extinction coefficient at 1250 M^{-1} cm^{-1} at 358.5 nm. The absorbance at 358.5 nm is due mainly to chlorine dioxide, but since the solution contained such a high chlorite ion concentration, the absorbance was corrected for chlorite ion.

A typical correction is approximately -0.050 absorbance units. The concentration of ozone in the original solution was calculated using the following equation:

$$\text{mg/L } O_3 = \frac{\text{Abs (corr.)}}{2.00 \text{ cm} \times 1250 \text{ M}^{-1} \text{ cm}^{-1}} \times \frac{5.366 \text{ ml}}{1.041 \text{ ml}} \times \frac{48000 \text{ mg } O_3}{1 \text{ mole } O_3} \times \frac{1 \text{ mole } O_3}{2 \text{ mole } ClO_2}$$

Reactions Between Chlorine Dioxide and Ozone. Chlorine dioxide was prepared using the persulfate ion method (27) and was collected in water at 2°C. The concentration of the stock solution was measured iodometrically. Dilute chlorine dioxide solutions were prepared by dilution with water and stored in a shrinking bottle. Typically, 0.504 ml 6.0×10^{-4} M chlorine dioxide solution was transferred from the shrinking bottle into the 2.00 cm cylindrical spectrophotometer cell which already contained 4.135 ml acetate buffer and a small teflon coated magnetic stir bar. A 1.041 ml aliquot of water was injected into the rapidly stirring chlorine dioxide. The cell was stoppered and the absorbance was measured at 358.5 nm. The reference cell contained 4.135 ml acetate buffer and 1.545 ml water. This measurement determined the "initial absorbance" which corresponds to the initial amount of chlorine dioxide.

The preceding experiment was repeated substituting the sample ozone solution for the aliquot of water. The measurement determined the "final absorbance" which corresponds to the amount of chlorine dioxide that had not reacted with the ozone. The difference between the initial absorbance and the final absorbance corresponds to the amount of chlorine dioxide that reacted with the ozone. The concentration of ozone in the original solution was calculated using the following equation:

$$\text{mg/L } O_3 = \frac{\text{Abs(init)-Abs(final)}}{2.00 \text{ cm} \times 1250 \text{ M}^{-1} \text{ cm}^{-1}} \times \frac{5.680 \text{ ml}}{1.041 \text{ ml}} \times \frac{48000 \text{ mg} O_3}{1 \text{ mole } O_3} \times \frac{1 \text{ mole } O_3}{2 \text{ mole } ClO_2}$$

**The volumetric measurement technique is detailed by Silverman, R.A., and Jordan, J., Journal Chemical Education, 50, 654, 1973.

BEGIN FIRST LINE OF TEXT HERE
CENTER OF PAGE
TOP OF IMAGE AREA
DROPPED HEAD; BEGIN SECTIONS HERE
BEGIN LAST LINE OF TEXT
3/8"
BOTTOM OF IMAGE AREA; OUTSIDE DIMENSION FOR TABLES AND ILLUSTRATIONS
EPA Form 2350-4 (4-80)
(PREVIOUSLY CIN. EPA FORM 237)
PAGE NUMBER
U.S. GOVERNMENT PRINTING OFFICE 1981-[illegible]
TYPING GUIDE SHEET

The Iron(II) Terpyridine Method

Preparation of Stock Iron(II) Indicator Solutions. Solutions 2.0×10^{-3} N in $Fe(phen)_3^{+2}$, $Fe(terpy)_2^{+2}$, and $Fe(5\text{-}NO_2\text{-}phen)_3^{+2}$ were prepared in one liter volumetric flasks by mixing 100 ml freshly prepared 2.0×10^{-2} M ferrous sulfate (5.5602 g $FeSO_4 \cdot 7H_2O$ per liter) with equivalent quantities of ligand and diluting to the mark with purified water. The exact weights of ligand are listed in Table 6 for the 2.0×10^{-3} N solution.

Solutions 2.0×10^{-4} N in the above indicators and containing excess ligand were prepared in 100 ml volumetric flasks by mixing 10 ml 2.0×10^{-3} N indicator solution with the quantity of free ligand listed in Table 6 for the 2.0×10^{-4} N solution and diluting to the mark with purified water.

TABLE 6. WEIGHT PREPARATIONS FOR IRON(II) INDICATOR SOLUTIONS

		2.0×10^{-3} N		2.0×10^{-4} N	
Ligand	MW	grams	moles/1000 ml	grams	moles/100 ml
Phen·H_2O	198.22	1.1892	0.006	0.0055	2.77×10^{-5}
Bipy	156.19	0.9373	0.006	0.0035	2.24×10^{-5}
Terpy	233.27	0.9331	0.004	0.0067	2.80×10^{-5}
5-NO_2-phen	225.20	1.3512	0.006	0.0050	2.22×10^{-5}

Preparation of Stock Ruthenium(II) Indicator Solutions. A solution 2.05×10^{-4} M $(Phen)_3RuCl_2$ and 2.1×10^{-4} M in phenanthroline was prepared in a 100 ml volumetric flask by dissolving 0.0146 g $(Phen)_3RuCl_2$ and 0.0041 g phenanthroline monohydrate in purified water.

A solution 2.15×10^{-4} M $(Bipy)_3RuCl_2$ and 2.0×10^{-4} M bipyridine was prepared as above by dissolving 0.0161 g $(Bipy)_3RuCl_2$ and 0.0032 g bipyridine in 100 ml purified water.

A solution 1.99×10^{-4} M $(terpy)_2RuCl_2$ and 2.6×10^{-4} M terpyridine was prepared by dissolving 0.01277 g $(terpy)_2RuCl_2$ and 0.0047 g terpyridine in 100 ml purified water.

A solution 2.05×10^{-4} M $(5\text{-}NO_2\text{-}phen)_3RuCl_2$ and 2.09×10^{-4} 5-nitrophenanthroline was prepared by dissolving 0.0174 g $(5\text{-}NO_2\text{-}phen)_3RuCl_2$ and 0.0047 g 5-nitrophenanthroline in 100 ml purified water.

BEGIN FIRST LINE OF TEXT HERE
CENTER OF PAGE
TOP OF IMAGE AREA
DROPPED HEAD BEGIN SECTIONS HERE
6-1/2"
BEGIN LAST LINE OF TEXT
3/8"
BOTTOM OF IMAGE AREA OUTSIDE DIMENSION FOR TABLES AND ILLUSTRATIONS
PAGE NUMBER
EPA Form 2350-4 (4-80)
(PREVIOUSLY CIN, EPA FORM 287)
TYPING GUIDE SHEET

Analytical Procedures. Prepare the indicator solution in a 100 ml volumetric flask: 10 ml stock indicator, 1 ml 3 N hydrochloric acid, and 10-20 ml purified water. For the baseline absorbance, A_o, fill to the mark with purified water. For an ozone determination, inject ozone sample into the indicator solution and dilute to the mark with purified water. Quickly mix the solution by inversion, transfer to a spectrophotometer cell and immediately read the absorbance at the appropriate wavelength.

$$\text{mg/L } O_3 = \frac{A_o - A}{E \cdot d} \times \frac{100}{V} \times 24000$$

where

A_o-A: difference in absorbance in the presence and absence of ozone

E: molar extinction coefficient

d: cell length

V: volume of ozone sample in ml

Preparation of Ruthenium(II) Complexes. The complexes $Ru(phen)_3^{+2}$, $Ru(bipy)_3^{+2}$, $Ru(terpy)_2^{+2}$ and $Ru(5\text{-}NO_2\text{-}phen)_3^{+2}$ were prepared by refluxing a mixture of 2.0 g $RuCl_3$ and stoichiometric amounts of the appropriate ligands for about three hours in 100 ml N,N-dimethylformamide (DMF) (28). At the end of three hours, the DMF was distilled off at atmospheric pressure until the solution volume was about 15 ml. This remaining solution was added slowly to 30 ml of a chilled saturated solution of tetraethyl ammonium chloride in reagent grade acetone. The brightly colored crystals were filtered and dried under vacuum.

The Iodate Method

In a 100 ml volumetric flask place sodium hydroxide, potassium iodide, sodium carbonate or sodium phosphate, iodine and enough water to bring the total volume to 25 ml. The flask was stoppered and lowered into a water bath at the appropriate temperature. After the reaction period sodium hydroxide and/or sodium carbonate or sodium phosphate was added to make the ionic background consistent between experiments and the solution diluted to 100 ml. A 40.00 ml aliquot was used for the iodate analysis. Sodium sulfite was added to facilitate removal of oxygen from the sample solution. This decreased the nitrogen bubbling time from 15 minutes to 5 minutes.

Enough iodine was initially added to the reaction flask to theoretically produce an iodate ion concentration of approximately 1.6×10^{-6} M after final dilution. This corresponds to an ozone concentration of approximately 2 mg/L.

A calibration curve based on standard potassium iodate in the appropriate ionic background was used to determine the iodate ion concentration in each experiment.

BEGIN FIRST LINE OF TEXT HERE
CENTER OF PAGE
TOP OF IMAGE AREA
DROPPED HEAD: BEGIN SECTIONS HERE
BEGIN LAST LINE OF TEXT
3/8"
BOTTOM OF IMAGE AREA; OUTSIDE DIMENSION FOR TABLES AND ILLUSTRATIONS
PAGE NUMBER
EPA Form 2350-4 (4-80)
(PREVIOUSLY CIN: EPA FORM 2571)
TYPING GUIDE SHEET

The Cerium Method

0.01 M Cerium(III) Sulfate in 1 N Sulfuric Acid. Place 7.13 g $Ce_2(SO_4)_3 \cdot 8H_2O$ (G. Frederick Smith Co.), purified water, and 57 ml concentrated sulfuric acid in a one liter volumetric flask. Stir until dissolved and dilute to the mark with purified water.

Standard Cerium(IV) Sulfate Solutions. Boil and stir 5.50 g ceric ammonium nitrate with 57 ml concentrated sulfuric acid for four hours in a beaker covered with a watch glass. Cool, pour into a one liter volumetric flask, rinse the beaker with 1 N sulfuric acid, and make up to the mark with 1 N sulfuric acid. The exact normality, 8.3488×10^{-3} N $Ce(SO_4)_2$, was determined by standardization against standard arsenic trioxide using osmium tetroxide as the catalyst and ferroin as the indicator.

To prepare the dilute working solution, 1.6698×10^{-4} $Ce(SO_4)_2$ in 1 N sulfuric acid, mix 20.00 ml 8.3488×10^{-3} N $Ce(SO_4)_2$ in 2 N sulfuric acid with 480 ml 2 N sulfuric acid in a one liter volumetric and dilute to the mark with purified water.

Analytical Procedure for Residual Ozone. Place 25 ml 0.01 M cerium(III) sulfate in 1 N sulfuric acid in a 100 ml volumetric flask. Add 10 ml sample of ozone solution and let sit for 10 minutes. Add 10.00 ml 2.0×10^{-4} M ferroin solution (containing 2.0×10^{-4} M excess free phenanthroline) and measure the absorbance at 510 nm. Calculate the ozone concentration by the decrease in absorbance in absence and presence of ozone as detailed in the ferroin procedures.

Analytical Procedure for Hydrogen Peroxide. Place 5.00 ml 1.6698×10^{-4} N cerium(IV) sulfate in 1 N sulfuric acid in a 100 ml volumetric flask. Add an aliquot of dilute hydrogen peroxide solution or an aliquot of "ozone" solution which has been purged of ozone by bubbling oxygen through the solution for 10-20 minutes. Let sit for 15 minutes, add 10.00 ml 2.0×10^{-4} M ferroin solution (containing 2.0×10^{-4} M excess free phenanthroline), dilute to mark, and measure the absorbance at 510 nm.

EPA Form 2350-4 (4-80)
(PREVIOUSLY CIN. EPA FORM 287)
TYPING GUIDE SHEET

SECTION 5

RESULTS AND DISCUSSION

Method Comparisons

The use of phenylarsine oxide (PAO) as a direct reductant for ozone requires that PAO (As(III)) is exclusively oxidized to phenylarsonic acid (As(V)) and that oxidation of the arsenic-carbon bond and the carbon-carbon double bonds are negligible because PAO decomposition would lower residual ozone measurements.

In the kinetic comparison shown in Figure 11, the two reductants were ozonized in acetate buffer pH 4.5, the pH was adjusted to 7 with 0.5 M sodium bicarbonate solution and the excess reductant back titrated with iodine to an amperometric endpoint (24). Although the PAO seems to be consistently high, the deviations are small enough to be within experimental error and the rate constants calculated by the FIT 80 program confirm the equivalence of PAO and arsenic(III) as direct reductants for ozone.

Smart reports that excess PAO may also be determined by differential pulse polarography (DPP) with a detection limit corresponding to 2.5 µg/l ozone (3).

Fig. 11 also illustrates the recurring and worrisome observation that in a kinetic comparison, one or two data points may fall significantly off the decay curve calculated by the FIT 80 program. Compare the experimental ozone concentrations determined by inorganic As(III) with the corresponding ozone concentration calculated from the decay curve (Table 7). For ten of the eleven points, the experimental and calculated ozone concentrations agree within 9%. The eleventh point, however, is 32.5% high. Single point deviations of this size frequently occurred in kinetic comparisons and they certainly make single point ozone analyses untrustworthy.

As shown in Table 8, PAO and sodium thiosulfate are equivalent when used in the amperometric method (24). Here both function as reductants for iodine and are not directly involved in an ozone reaction. When these amperometric method results are compared with the results from As(III) direct oxidation, however, the ozone concentration determined by As(III) direct oxidation are 9% low. Thus, when the ozone reductant changes from iodide ion to arsenic(III), a difference occurs.

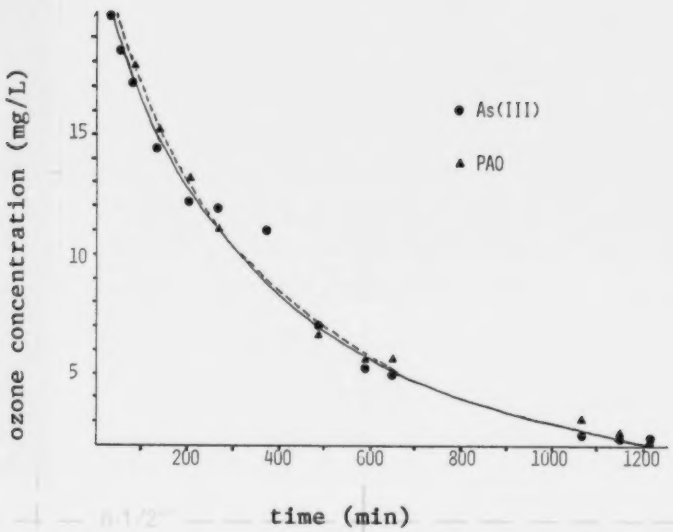

Figure 11. Comparison of As(III) and PAO as Direct Reductants.

TABLE 7. COMPARISON OF EXPERIMENTAL AND CALCULATED OZONE CONCENTRATION FOR INORGANIC As(III) AS DIRECT REDUCTANT

mg/L O_3	
Experimental	Calculated
21.7	21.7
19.9	19.7
18.5	18.3
14.5	14.3
12.2	12.0
11.0	8.3
5.3	5.5
5.0	5.0
2.4	2.6
2.5	2.3
2.2	2.1

TABLE 8. COMPARISON OF PAO AND SODIUM THIOSULFATE IN THE AMPEROMETRIC METHOD ALONG WITH A COMPARISON OF THE AMPEROMETRIC METHOD WITH As(III) DIRECT OXIDATION

Amperometric		As(III) Direct
PAO	$Na_2S_2O_3$	pH 4 - 4.5
14.5 ± .3 mg/L	14.8 ± .3 mg/L	13.5 ± .1 mg/L

The DPD and the arsenic(III) back titration methods differ significantly in the excess reagent present when ozone oxidizes iodide ion to iodine and in the iodine quantification. In the arsenic(III) back titration, ozone could be directly reduced by arsenic(III). Although this reduction occurs at a much slower rate than reduction by iodide ion, but the stoichiometry of one ozone per one arsenic(V) is maintained. In the DPD method ozone could oxidize DPD or the Wurster cation to the diimine cation and these direct attacks of ozone on the indicator would lead to low results. The DPD calibration curve is based on standard iodine and the iodine quantification should not be responsible for differences between the methods.

A kinetic comparison of the DPD and the arsenic(III) back titration methods in purified water (Fig. 12) shows considerable scatter and illustrates the importance of the kinetic technique. If conclusions had to be based on single point comparisons, then the first, second, and third data point sets would lead to three different conclusions. Figures 13 and 14 are the ozone decay curves in purified water spiked with 4.8 mg/L hydrogen peroxide prior to ozonation and the ozone decay curves in tap water, respectively. Scatter decreases as the radical scavenger concentration increases. Fig. 14 clearly confirms the equivalence of the DPD method and the arsenic(III) back titration method.

The DPD method is not equivalent to the Indigo method as shown by the decay curves for ozone in purified water (Fig. 15). The DPD points are scattered and ozone concentrations are low compared to the smooth Indigo plot. The critical differences between these two methods are ozone reduction by a carbon-carbon double bond at pH 2 and ozone reduction by iodide ion at pH 6.4. Iodate ion formation could be responsible for the low DPD titer. Iodate ion formation is also indicated in comparisons made using the Iodometric method at pH 3.5, 5, 7, 9 and the arsenic(III) direct oxidation method in bicarbonate ion solution at pH 7 (Tables 9 and 10) (29). Least squares analyses of plots of the Iodometric method results on the x-axis vs. the arsenic(III) direct oxidation results on the y-axis are shown in Table 9.

The positive Y-intercepts of Table 9 show that the arsenic(III) direct oxidation method consistently gives low results. The slope shows the trend that the Iodometric method gives lower results as the pH increases. This error is consistent with iodate ion formation and with hydrogen peroxide formation. It also implies, however, that iodate ion is not quantitatively reconverted to iodine under the acidic titration conditions.

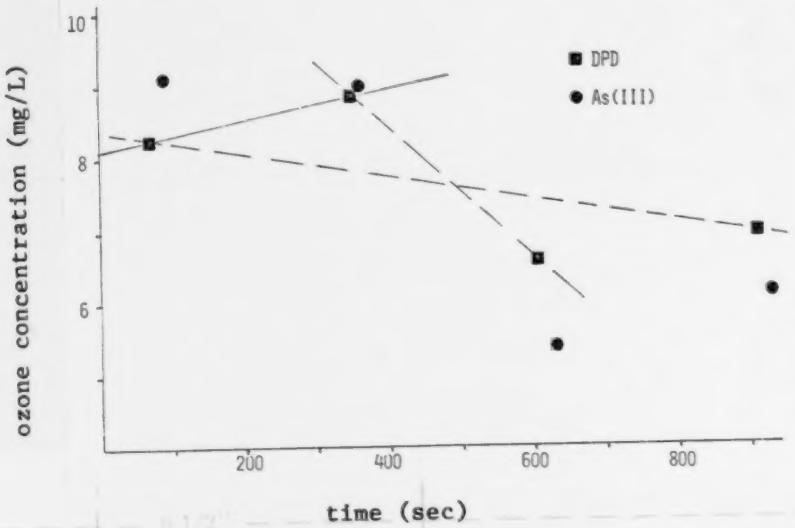

Figure 12. Comparison of DPD and As(III) Back Titration in Purified Water.

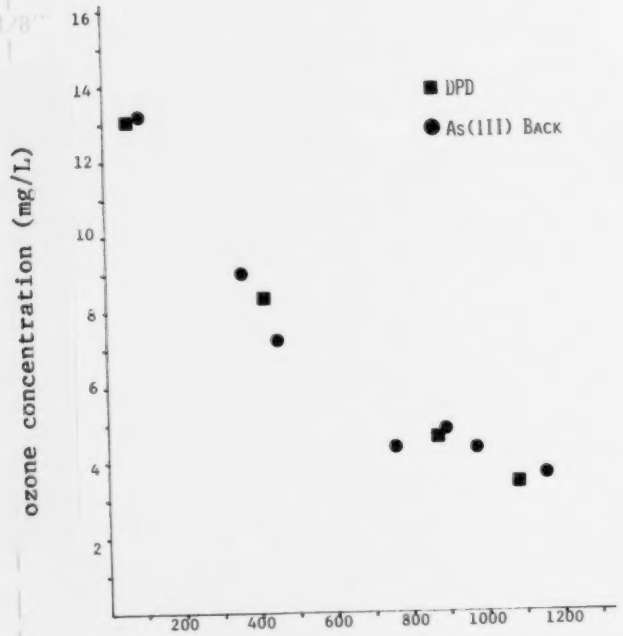

Figure 13. Comparison of DPD and As(III) Back Titration in Purified Water with 4.8 mg/L H_2O_2.

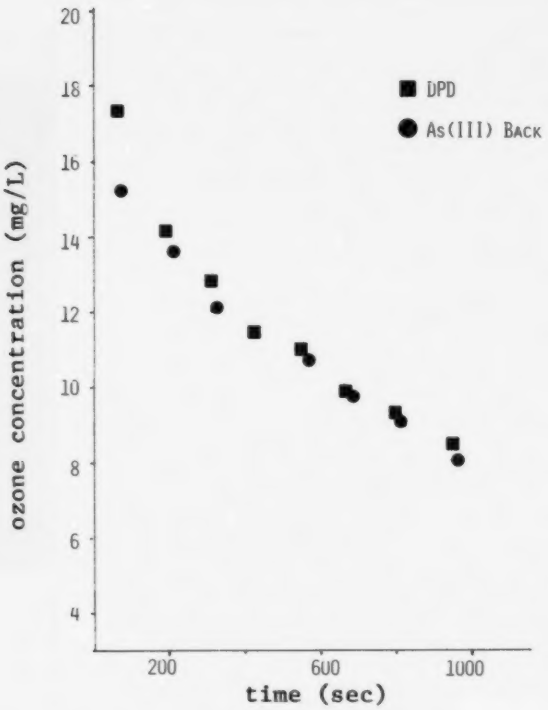

Figure 14. Comparison of DPD and As(III) Back Titration in Tap Water.

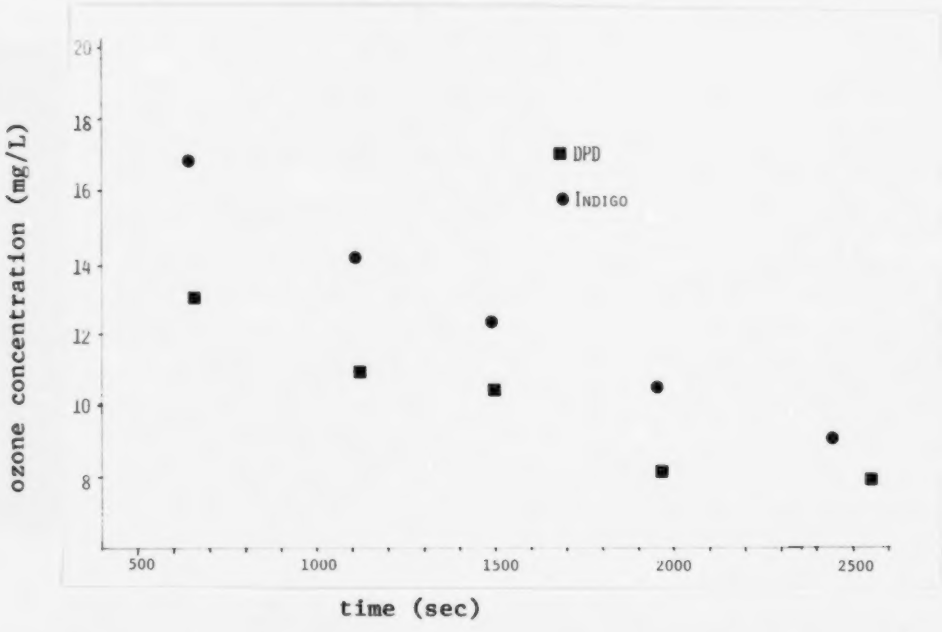

Figure 15. Comparison of DPD and Indigo in Purified Water.

TABLE 9. IODOMETRIC (pH 3.5 - 9.0) vs. As(III) DIRECT (pH 7.0)

pH	Y-intercept	slope	correlation
3.5	0.95	1.00	0.9998
5.0	0.88	0.89	0.9979
7.0	0.95	0.70	0.9947
9.0	0.74	0.81	0.9986

TABLE 10. COMPARISON OF IODOMETRIC METHOD AND ARSENIC(III) DIRECT OXIDATION

Iodometric mg/L O_3	As(III) Direct Oxidation mg/L O_3
pH 3.5 Acetate	
7.44	6.53
9.54	8.50
15.50	14.30
22.10	21.20
pH 5 Boric Acid	
2.20	1.35
2.54	2.02
7.82	7.61
10.20	10.10
10.30	10.80
15.50	17.4
22.10	23.3
pH 7 Phosphate	
7.85	8.96
5.92	6.86
12.90	17.3
11.00	14.7
9.11	11.1
4.12	5.02
2.95	3.20
pH 9 Borate	
3.50	3.24
4.86	5.12
6.13	6.71
7.79	8.71
9.53	11.10
11.0	12.40

Iodate Ion Formation

The formation of iodate ion was measured for the ozone oxidation of 2% iodide ion solutions in 0.1 M phosphate buffers at pH 7.3, 6.8, 5.3, 2.2. Immediately after the ozone injection, standard arsenic(III) was added and two aliquots were removed: one for iodate ion analysis and the other for ozone analysis by the back titration of excess arsenic(III). All iodate ion aliquots were immediately made strongly basic for differential pulse polarographic (DPP) analysis and the back titration aliquots at pH 5.3 and 2.2 were brought to neutrality with sodium hydroxide. The DPP analysis is capable of detecting an iodate ion concentration as low as 1 x 10-8 M (30,31). This corresponds to 0.001 mg/L ozone taking into account the 3:1 ozone:iodate ion stoichiometry. As expected, iodate ion formation tends to increase with ozone concentration and with pH. The largest iodate ion concentration was found at pH 7.3 and corresponded to 0.265 mg/L ozone. No iodate ion was detected at pH 2. (Table 11). The iodate ion concentrations are too low to explain the observed differences in the ozone decay curves traced by the arsenic(III) back titrations and by the Indigo method (Fig. 16).

TABLE 11. IODATE ION FORMATION

pH 2.2	pH 5.3		pH 6.8		pH 7.3	
time	mg/L O_3	time	mg/L O_3	time	mg/L O_3	time	mg/L O_3
None	90	0.176	74	0.147	26	0.173
	280	0.143	240	0.107	197	0.234
	510	None	500	0.091	420	0.100
	755	0.058	745	0.100	685	0.265
	1035	None	985	0.058	900	0.078
	1565	None	1555	None	1485	0.109

Fig. 17 shows the ozone decay curves determined when the above experiment was repeated for pH 7.0 and pH 2.0 with arsenic(III) present in the iodide ion solution during the ozone addition. Iodate ion concentrations corresponding to less than 0.024 mg/L ozone were found at pH 7 and no iodate ion was detected for pH 2 (Table 12). Therefore, when an ozone solution containing less than 14 mg/L is added directly to iodide ion (without the use of a glass frit), iodate ion formation is not sufficient to significantly interfere with ozone analysis.

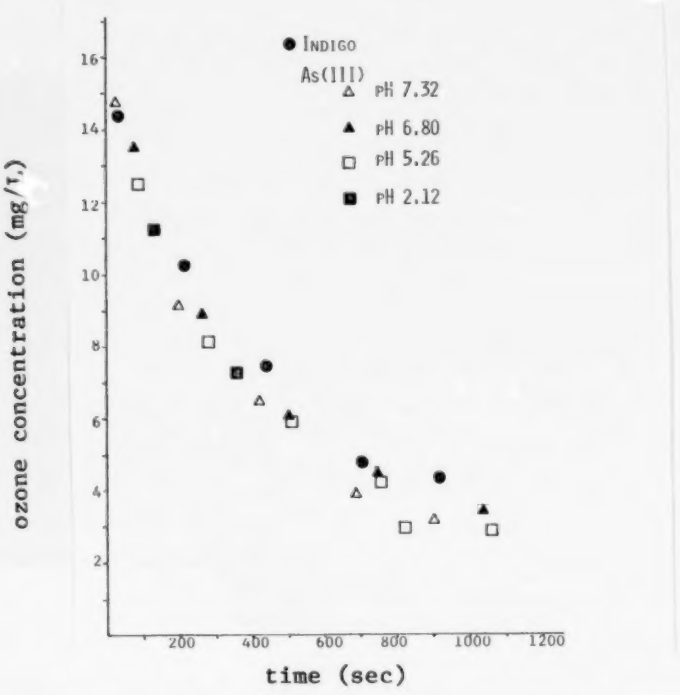

Figure 16. Comparison of Indigo and As(III) Back Titration in Phosphate Buffer pH 7.21.

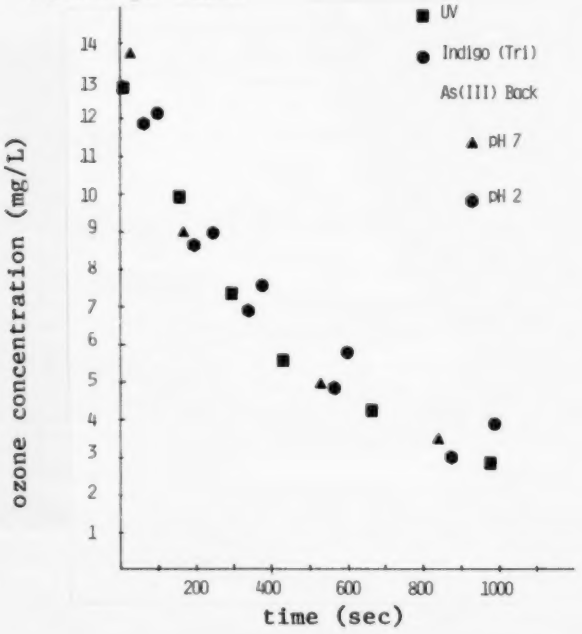

Figure 17. Comparison of UV, Indigo and As(III) Back Titration in Phosphate Buffer pH 7.2

TABLE 12. IODATE ION FORMATION pH 7

time (sec)	mg/L O_3
29	0.024
230	0.023
490	0.021
842	0.014
1155	None

Hydrogen Peroxide Formation

Hydrogen peroxide can be formed by the ozone-iodide ion redox reaction and by the decomposition of ozone in water. Its concentration, measured by DPP after one hour ozonation of 0.07 M phosphate buffers, varied with pH and with exposure to UV light (Ace Hanovia high pressure mercury vapor lamp). The detection limit of 1×10^{-7} M corresponds to 0.0034 mg/L. In the absence of UV light, the hydrogen peroxide level increases with pH (Table 13) and in the presence of UV light the hydrogen peroxide level decreases with an increase in pH (Table 14).

TABLE 13. HYDROGEN PEROXIDE FORMATION WITH OZONE DECAY

pH	$[H_2O_2] \times 10^7$ M
2.05	4.84
7.05	7.07
12.00	10.0

TABLE 14. EFFECT OF UV ON HYDROGEN PEROXIDE FORMATION WITH OZONE DECAY

pH	$[H_2O_2] \times 10^7$ M	$[H_2O_2] \times 10^7$ M with UV
7.0	2.9	9.5
11.8	4.0	8.7
7.8		77.9
11.8		4.7

The large variations in the hydrogen peroxide concentrations in the two tables shows that the hydrogen peroxide concentration varies dramatically under seemingly similar conditions. All the hydrogen peroxide titers are too small to account additively for method/pH differences. The hydrogen peroxide probably catalyzes ozone decomposition since at 10^{-7} M hydrogen peroxide the hydroperoxyl anion is as important as hydroxide ion as a catalyst (26).

Buffer Effects

The scatter observed in kinetic comparisons of ozone decay in purified water is reduced by working with ozone in buffered purified water. Because this is a trend with all methods, the significant difference must lie in the ozone solution. A comparison of the Indigo method, arsenic(III) back titration and arsenic(III) direct oxidation methods on ozone decay in purified water buffered to pH 6.7 with perchloric acid-phosphate mixtures shows the three methods to be alike. (Fig. 18 and 19). Scatter varies significantly between the two runs. The only intentional change in the runs was the length of time ozone bubbled through the contactor solution: 30 min. for Fig. 18 and 60 min. for Fig. 19 (less scatter).

The ozone decay curves by the Indigo method, by direct UV measurement, and by arsenic(III) direct oxidation method (pH 6.8 phosphate) for ozone in purified water buffered to pH 7.7 with a KH_2PO_4-NaOH mixture, however, show the Indigo method and UV method to give higher residual ozone concentrations than the arsenic(III) direct oxidation method. (Fig. 20).

When the Indigo method, the direct UV measurement, and the arsenic(III) direct oxidation method are compared on acidified ozone solutions undergoing minimal decay, they are equivalent. (Fig. 21).

Causes for Method Differences

The kinetic technique has revealed differences among methods. These variations could be caused by:

1) the reaction of ozone or ozone decay products with the oxidized indicator (e.g. iodate formation).

2) the reaction of ozone decay products with the reductant or indicator.

3) the further decomposition of ozone before reaction with the reductant. This could be caused by the pH of the reductant solution, solutes in the reductant solution, or by a relatively slow reaction between ozone and reductant.

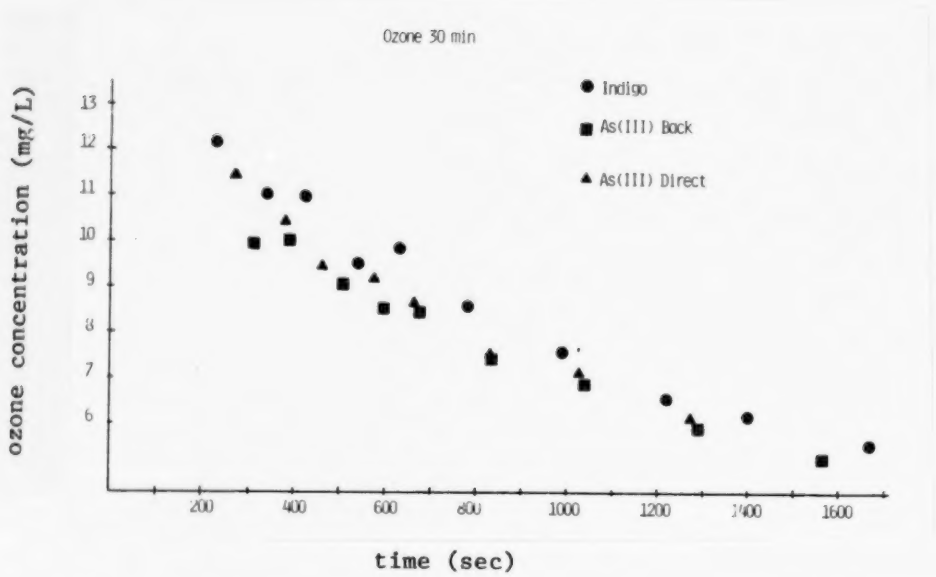

Figure 18. Comparison of Indigo, As(III) Back, and As(III) Direct in Phosphate Buffer pH 6.7 : Ozone 30 min.

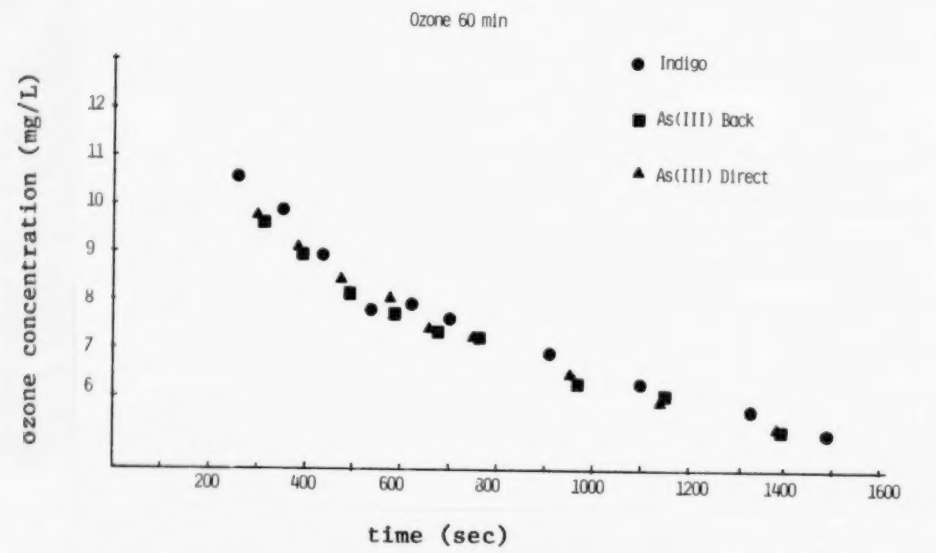

Figure 19. Comparison of Indigo, As(III) Back, and As(III) Direct in Phosphate Buffer pH 6.7 : Ozone 60 min.

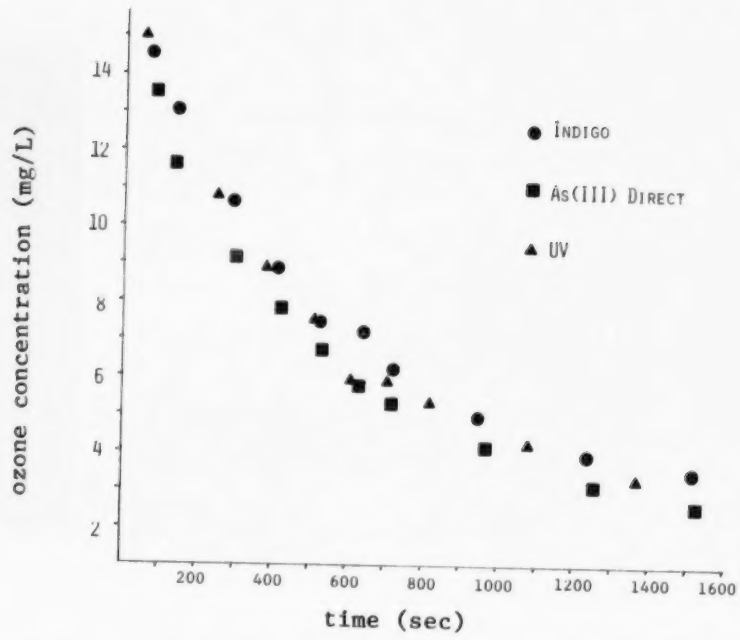

Figure 20. Comparison of Indigo, As(III) Direct, and UV in Phosphate Buffer pH 7.7.

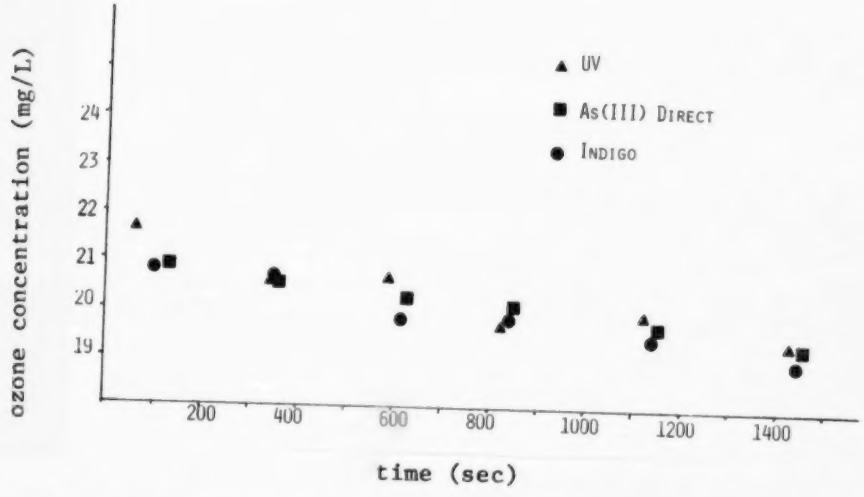

Figure 21. Comparison of UV, As(III) Direct, and Indigo in Phosphoric Acid pH 2.3.

Hydrogen Peroxide Effect

The effect of the addition of hydrogen peroxide on the residual ozone titer was examined. Oxford tap water was ozonated, acidified for stabilization, and analyzed for residual ozone by UV analysis, the Indigo method, the direct oxidation of arsenic(III) in neutral phosphate buffer, and the back titration of arsenic(III). Next, the residual ozone titer was determined with the addition of 3 mg/L hydrogen peroxide to the reductant solution immediately prior to ozone sampling (Table 15).

TABLE 15. EFFECT OF HYDROGEN PEROXIDE ON CONCENTRATION OF RESIDUAL OZONE

Method	mg/L O_3	mg/L O_3 H_2O_2
UV	8.98 ± 0.05	8.79 ± 0.12
Indigo	9.52 ± 0.45	9.11 ± 0.05
As(III) (direct)	9.42 ± 0.23	9.32 ± 0.04
As(III) (back)	11.62 ± 0.20	12.22 ± 0.27

The arsenic(III) back titration method gives a residual ozone level 2.64 mg/L or 29% higher than the UV method for analyses on acid stabilized ozone solutions. Hydrogen peroxide increased this error to 3.43 mg/L or 39% for the arsenic(III) back titration method. The Indigo and arsenic(III) direct oxidation titers agreed within 6% of the UV titers.

Ozone decomposition prior to reaction with the reductant is most likely to complicate the arsenic(III) direct oxidation method due to the relatively slow reduction of ozone by arsenic(III). Iodide ion reduces ozone in a virtually diffusion controlled reaction. The Indigo reductant solution is buffered at pH 2 eliminating ozone decay prior to attack of the carbon-carbon bond. In fact, when an arsenic(III) back titration reductant solution is dosed with concentrated ozone, the amber iodine color appears immediately and then fades as the iodine reacts with the arsenic(III). This clearly demonstrates that the ozone reacts faster with iodide ion than with arsenic(III). When a dilute ozone solution undergoing minimal decay was directly reduced by arsenic(III) in acetate buffer pH 4.5 and in phosphate buffer pH 6.8, both arsenic determined decay curves were scattered compared with the UV curve. The acetate curve had wide deviations from the calculated curve (Fig. 22). The residual ozone concentrations for three steady state solutions were also determined by these methods and compared with the concentrations determined by the direct oxidation of arsenic(III) in unbuffered solution at pH 7 (Table 16). The ozone titers do not consistently increase with a decrease in pH and the ozone titers determined in unbuffered arsenic(III) are low relative to buffered solutions and the UV method.

TABLE 16. COMPARISON OF BUFFERS FOR As(III) DIRECT REDUCTION

mg/L RESIDUAL OZONE

	pH 4.5	pH 6.8	pH 7
UV	Acetate	Phosphate	No Buffer
6.62 ± .19	6.13 ± .14	6.42 ± .04	5.92 ± .27
7.00 ± .29	7.04 ± .01	6.64 ± .01	6.34 ± .01
9.06 ± .05	8.91 ± .33	8.81 ± .21	8.49 ± .06

Ozone Decay

If ozone decay prior to reduction by arsenic(III) causes low ozone titers, then any change in the reductant medium to slow decay should increase the ozone titer. As generally accepted and as illustrated in Fig. 23, the rate of ozone decay decreases with decreasing pH. These rates were determined by direct UV measurement in 0.1 M phosphate buffers ranging in pH from 9.4 to 5.9.

Ozone decay, however, is a complex function of pH and solutes. The relative rates for ozone decay in solutions at pH 7.0 -7.2 containing varying concentrations of phosphate and carbonate ions are listed in Table 17.

TABLE 17. EFFECT OF PHOSPHATE AND CARBONATE IONS ON OZONE DECAY

pH 7.0 - 7.2 k_2 obs x 10^6

		[carbonate] 0.0 M	0.01 M	0.1 M
[phosphate]	0.0 M	200	2.2	2.4
	0.1 M	38	2.6	2.0
	0.25 M	22	6.0	5.3
	0.50 M	46	10	8.4

These anions exert an enormous effort. The $t_{1/2}$ for purified water containing no phosphate or carbonate and adjusted to pH 7.0 with sodium hydroxide, is less than 500 sec. The $t_{1/2}$ in 0.1 M phosphate, 0.01 M carbonate is longer than 12 hours.

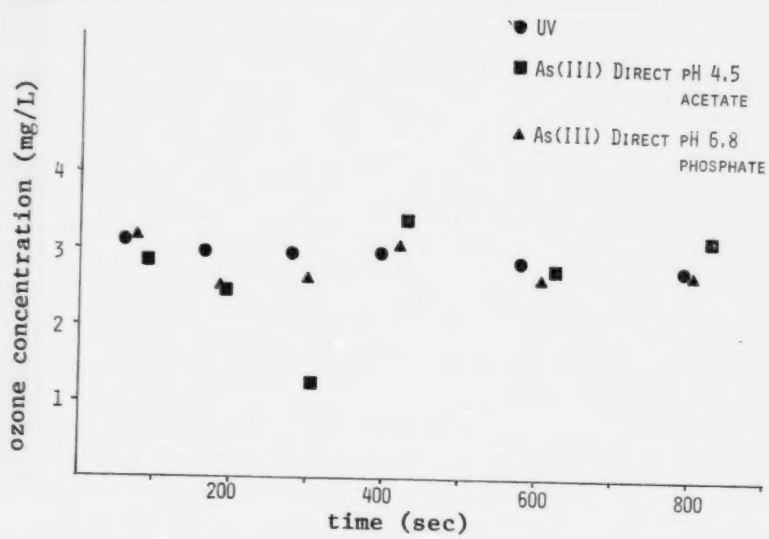

Figure 22. Comparison of UV, As(III) Direct (pH 4.5 acetate) and As(III) Direct (pH 6.8 phosphate) in Purified Water.

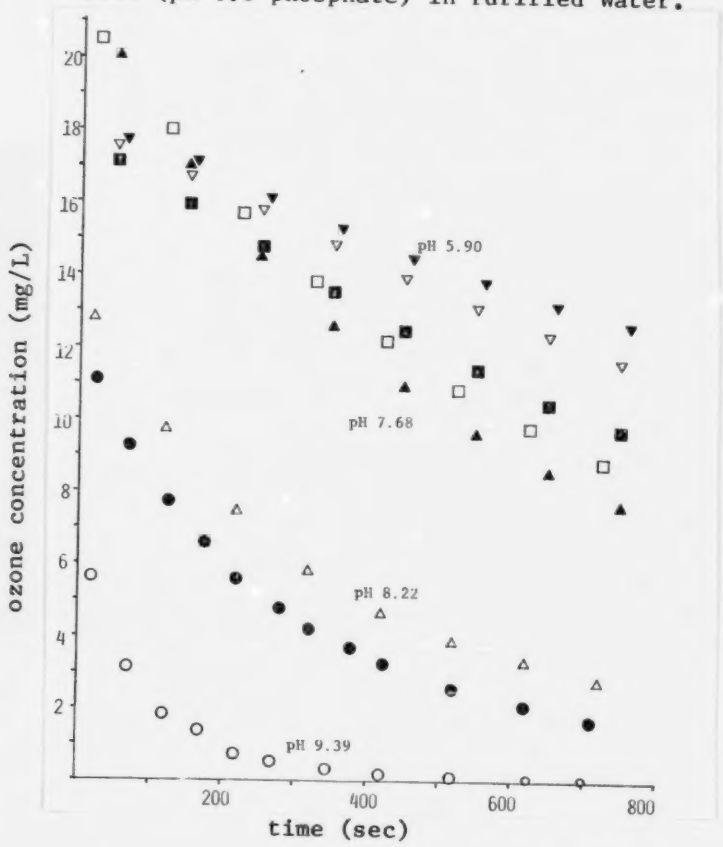

Figure 23. Effect of pH on Ozone Decay in Phosphate Buffer.

Purging Technique

The experiments reported here clearly demonstrate that the purging technique--widely used in order to eliminate *in situ* interferences--is unreliable because of ozone decomposition during the purge and readsorption steps and because of titer changes occurring in the acidified iodide ion solution throughout the readsorption step.

The Indigo method was evaluated by the purging technique on low concentration ozone solutions stabilized with phosphoric acid. These are ideal conditions for the purging technique because ozone decay is minimized and because the ozone indigo titer is stable despite the time delay necessitated by the purging interval. A 3-4 mg/L acidified ozone solution was prepared in the contactor and the exact ozone concentration determined by direct UV measurement (contactor-UV). One aliquot of this ozone solution was added to an indigo solution as usual and the ozone titer determined as usual (indigo-liq). A second aliquot was placed in an impinger tube and the ozone was purged by an oxygen stream through a bubbler into an indigo solution (indigo-gas). After ten minutes of purging, the ozone remaining in the impinger was determined by direct UV measurement (impinger-UV). Two types of bubbler tips were tested--a medium porosity frit and a capillary tip. The results are summarized in Table 18.

TABLE 18. EVALUATION OF THE PURGING TECHNIOUE WITH THE INDIGO METHOD ON ACID STABILIZED OZONE SOLUTIONS

	mg/L Ozone		
	Run 1	Run 2	Run 3
Contactor UV	3.12	3.31	2.96
Indigo Liq	3.29	3.37	3.38
Indigo Gas Frit Tip	3.37	2.57	4.21
Impinger UV	--	.261	.329
Contactor UV	3.01	3.10	3.00
Indigo Liq	3.31	3.37	3.33
Indigo Gas Capillary Tip	1.14	0.93	0.86
Impinger UV	0.180	0.144	0.102

Clearly the capillary tip is inadequate and the ozone bubbles through the indigo solution and escapes to the air prior to reaction. The frit tip looked promising and a second series of comparisons were run. These numbers summarized in Table 19 revealed the ozone concentrations determined by indigo-gas and by indigo-gas plus impinger UV to be consistently lower than both the contactor UV and the indigo-liq ozone concentrations. The only known experimental difference between the first evaluation which gave reasonably good agreement between the indigo-liquid and the indigo-gas ozone titers and this second evaluation which gave indigo-gas ozone titers significantly lower than the indigo liquid ozone titers was the moisture level in the bubbler tube. The first ozone sample "bumped" during the purge and the bubbler tube had to be rinsed. The moisture probably catalyzed ozone decomposition.

Whatever the reason for the low Indigo gas ozone titers, these experiments run under ideal conditions for the ozone purging technique reveal great caution must be used with the purging procedure.

TABLE 19. EVALUATION OF THE PURGING TECHNIQUE WITH THE INDIGO METHOD ON ACID STABILIZED OZONE SOLUTIONS

mg/L ozone			
contactor UV	Indigo liq	Indigo gas frit tip	Impinger UV
4.04	4.18	--	--
3.90	4.32	3.28	0.08
3.72	4.01	3.17	0.41
3.69	4.32	3.68	0.46
3.84	4.25	3.04	0.11
3.94	4.24	3.08	0.12

Delta Electrode

The Delta amperometric membrane electrode measures ozone concentrations in situ and should not be influenced by ozone instability or overoxidation. A teflon membrane selectively transports gaseous molecules like ozone to the cathode and prevents transfer of polar species and ions. The electrode operates at a potential where only very strong oxidants are reduced. Thus, the Delta electrode promises the ideal combination of chemical selectivity and the capability for continuous monitoring. To be practical, the electrode must be easily calibrated, must remain calibrated for a reasonable length of time, perhaps a minimum of one working day, and the calibration must be valid over the working range of the electrode, 0-10 mg/L. Direct UV measurement of ozone was used to calibrate the electrode.

The kinetic comparison of ozone decomposition by direct UV measurement, the Indigo method, and the Delta electrode shown in Fig. 24, illustrates two recurring problems. First, ozone decay determined by the Delta electrode followed its own rate law. Second, the electrode rarely maintained calibration on switching from one solution to another. The initial points of Fig. 24 are low for this reason.

The change in rate law was traced to the lack of linear response of the electrode over a large concentration range. The electrode was calibrated by UV analyses on an acidified ozone solution. A volume of this solution was removed and replaced with an equal volume of acidified water and the electrode response and UV absorbance measured. This dilution was repeated several times to obtain stable ozone solutions of varying concentration within a 2.5 hour period.

The results in Table 20, 21, 22 and 23 show that as the ozone concentration decreases relative to the calibration concentration, the error increases. With the original electrode purchased from Delta Scientific (electrode 1), a 102.2% error is observed over a concentration range of 6.75 mg/L and this error drops to 19.1% for a concentration change of 3.46 mg/L (Table 20).

TABLE 20. ELECTRODE 1. DILUTION EXPERIMENT 1 FOR LINEAR RESPONSE

mg/L UV	mg/L Electrode	Error
8.60 ± 0.23	8.69 ± 0.06	
6.67 ± 0.17	7.43 ± 0.13	11.4%
5.14 ± 0.17	6.12 ± 0.13	19.1%
3.85 ± 0.10	6.17 ± 0.05	34.3%
2.64 ± 0.06	4.36 ± 0.05	65.2%
1.85 ± 0.04	3.74 ± 0.07	102.2%

TABLE 21. ELECTRODE 1. DILUTION EXPERIMENT 2 FOR LINEAR RESPONSE

mg/L UV	mg/L Electrode	Error
7.31 ± 0.05	7.38 ± 0.07	
5.77 ± 0.12	6.60 ± 0.01	14.4%
4.33 ± 0.09	5.81 ± 0.06	34.2%
3.35 ± 0.06	5.13 ± 0.05	53.1%
2.54 ± 0.04	4.47 ± 0.05	76.0%

TABLE 22. ELECTRODE 1. DILUTION EXPERIMENT 3 FOR LINEAR RESPONSE

mg/L UV	mg/L Electrode	Error
3.58 ± .04	3.67	2.5%
2.78 ± .06	3.05	9.9%
2.04 ± .07	2.30	12.6%
1.49 ± .03	1.68	12.9%
1.00 ± .03	1.16	16.1%
0.72 ± .03	0.85	18.4%
0.53 ± .02	0.68	27.6%

TABLE 23. ELECTRODE 2. DILUTION EXPERIMENT 4 FOR LINEAR RESPONSE

mg/L UV	mg/L Electrode	Error
4.03 ± .04	4.00	-0.7%
3.80 ± .08	3.75	-1.2%
2.65 ± .05	2.55	-3.5%
1.86 ± .03	1.91	2.5%
1.30 ± .02	1.46	12.8%
0.84 ± .01	0.99	17.7%
0.54 ± .01	0.67	22.7%
0.30 ± .02	0.50	66.4%
0.16 ± .01	0.33	107.6%

Improvements in electrode design promise to expand the useful linear range. The original electrode 1 measured ozone concentrations over a 2.1 mg/L range with 13% error while a second electrode, electrode 2, generously loaned by Delta Scientific, measured ozone concentrations with 2.5% error over this range.

In order to test the ability of the electrode to maintain calibration, the electrode, once calibrated by UV analysis on an acid stabilized ozone solution, was used to determine residual ozone in freshly prepared solutions of ozone over five days. The results are summarized in Table 24. Clearly, the electrode requires calibration for each run.

TABLE 24. ELECTRODE 1. CALIBRATION STABILITY OF THE DELTA ELECTRODE

Day	UV mg/L O_3	Electrode mg/L O_3	Error
1	4.5	4.5	
1	4.6	4.2	-8.7%
1	5.1	5.3	+3.9%
2	3.4	3.3	-2.9%
2	6.3	5.0	-20.6%
2	3.5	3.0	-14.3%
3	7.2	5.5	-23.6%
4	7.5	5.2	-30.7%
5	5.3	3.5	-34.0%

In a kinetic comparison, Oxford waste water was ozonated for 10 minutes and the residual ozone concentrations were determined over the next 15 minutes by the Indigo method, the arsenic(III) back titration method, the arsenic(III) direct oxidation method, and the Delta electrode (electrode 2). The waste water was then reozonated for 15 minutes and the decay followed as above. Results are shown in Fig. 25. The decay curve traced by Delta electrode 2 differs from the other methods and the electrode again appears to have lost calibration between runs. This instability and unpredictability of the Delta electrode clearly emphasize the necessity for recalibration for each run.

Ozone Decay in Waste Water

In Fig. 25 notice that the second decay curve traced by the Indigo method and the arsenic(III) back titration and arsenic(III) direct oxidation methods is very similar to the first curve. This was a consistent observation in sequential ozonation experiments with Oxford waste water. For example, in Fig. 26 one curve represents ozone decay following an initial 30 min. ozone treatment. This was followed on the next day by a two hour ozone treatment for which the ozone decay curve was not determined. Finally on the third day, a 30 min. ozone treatment was repeated and the ozone decay followed. This decay curve is included in Fig. 26. The similarity between the two decay curves is striking.

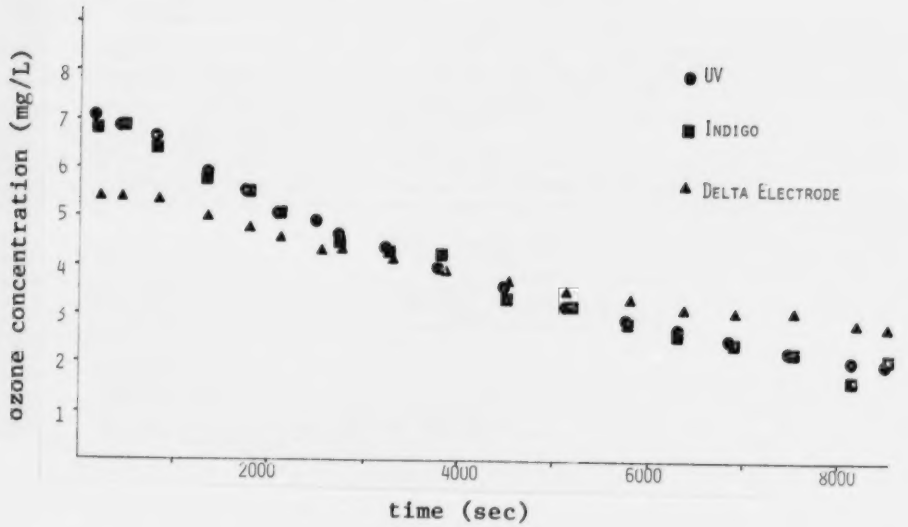

Figure 24. Comparison of UV, Indigo and Delta Electrode in Purified Water.

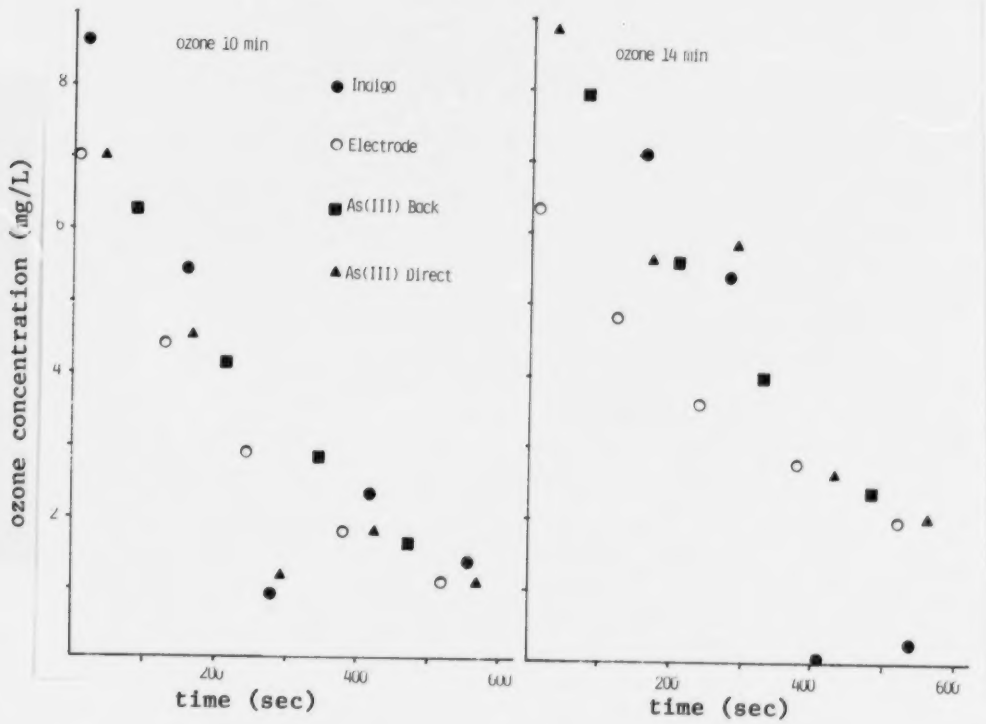

Figure 25. Comparison of Indigo, Delta Electrode, As(III) Back and As(III) Direct in Waste Water.

The ozone decomposition rate was also similar after each of 5 min. consecutive ozone treatments on Oxford waste water (Fig. 27). These experiments imply that once ozone satisfies the initial ozone demand of waste water, residual ozone levels are controlled by ozone self decomposition and not by direct reaction with impurities. Making the reasonable assumption that sufficient radical scavengers are present to quench the first order decay process, the residual ozone decay should be pH controlled.

The pH controlled decay rate can be measured by determining the ozone $t_{1/2}$ at a given pH with increasing concentrations of radical scavengers. The $t_{1/2}$ should reach a limiting value for each pH. With knowledge of the pH of the ozonated effluent and the maximum $t_{1/2}$ at this pH, showing the presence of ozone after a calculated time could be sufficient to assure disinfection.

The validity of the above hypothesis should be tested by determining the ozone doses and contact times necessary at various pH's to disinfect waste waters containing substances other than the organisms to be killed. The results of these tests would allow proper disinfection without the waste of overapplication of ozone. In addition, minimal ozone application increases efficiency and decreases cost and negative environmental effects.

New Reductant Systems

Reliable and practical procedures that treatment plant operators can use routinely are essential. The present sampling precautions, the stringent cleaning of glassware and the time restraints are unlikely to be appreciated by most plant operators. Therefore, new reductant systems for ozone were investigated over the course of this project to overcome the drawbacks of the published methods. The objective was to discover a reductant system that would be selective for very strong oxidants, that would produce a stable ozone titer, and that would require minimum instrumentation. A system that could function as a continuous and automatic monitor for residual ozone would be ideal because the monitor could control the ozone generator.

The systems explored were chlorite-chlorine dioxide, ferroins-ferriins, iodide-iodate, and cerium(III)-cerium(IV). Each of these systems ultimately failed as an analytical method but each in early and limited testing looked promising. The rationales, the results, and the probable flaws in each of these four methods are discussed below.

Chlorite Ion Method

The large reduction potentials of oxychlorine species indicate that chlorite ion (ClO_2^-) and chlorine dioxide (ClO_2) should be selective reductants for ozone.

$$HClO_2 \rightarrow ClO_2 + H^+ + e^- \qquad E^\circ = -1.27v$$

$$ClO_2 + H_2O \rightarrow ClO_3^- + 2H^+ + e^- \qquad E^\circ = -1.15v$$

$$HClO_2 + H_2O \rightarrow ClO_3^- + 3H^+ + 2e^- \qquad E^\circ = -1.21v$$

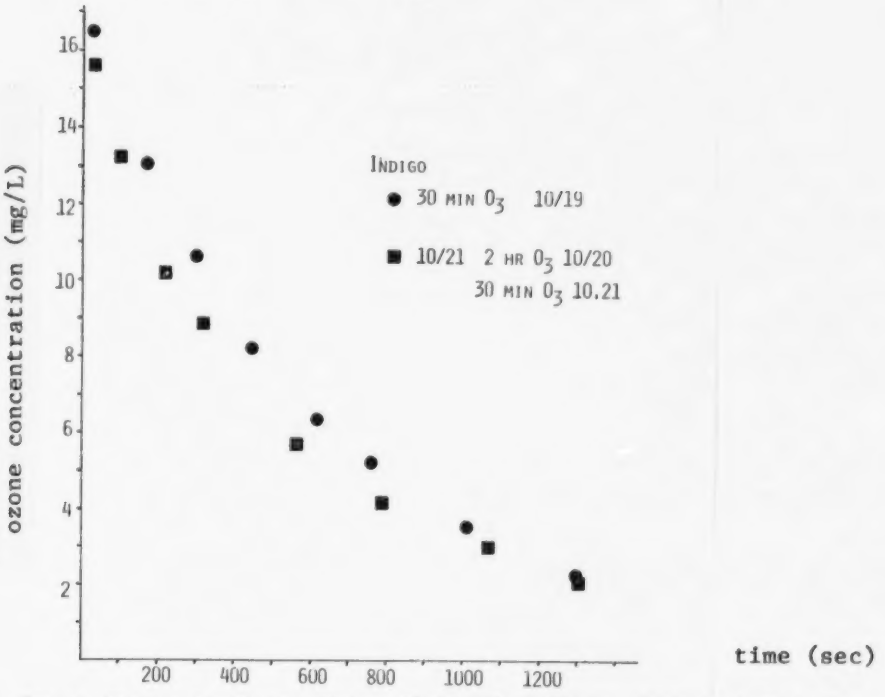

Figure 26. Ozone Decay in Waste Water Following Three Sequential Ozone Treatments.

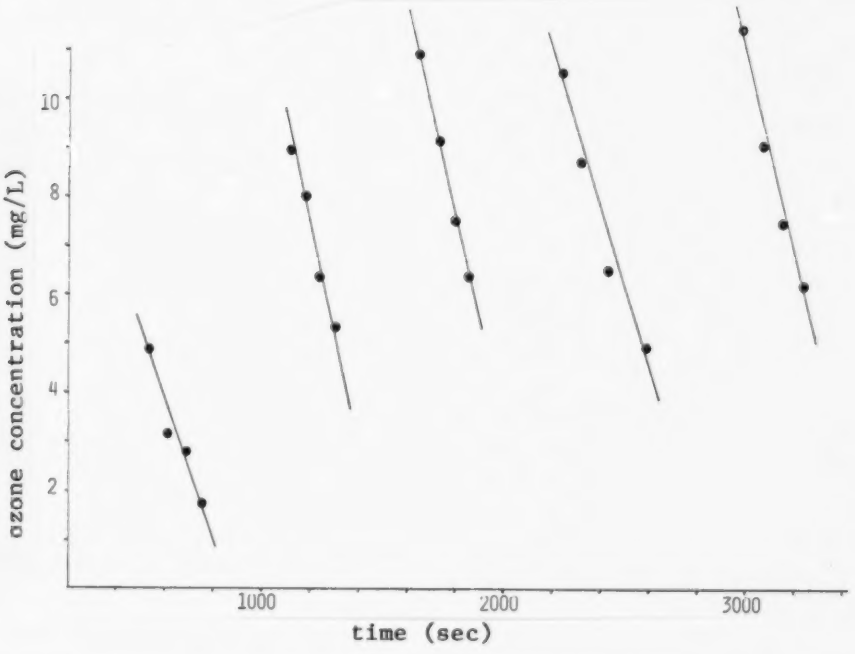

Figure 27. Ozone Decay in Waste Water Following Five Sequential Ozone Treatments.

Any chlorine based system also offers the two advantages that (1) chlorine and oxychlorine species are well documented and that (2) all United States water laboratories are equipped for chlorine/oxychlorine chemistry.

Theoretically ozone can oxidize chlorite ion to chlorine dioxide. Then in a second step, the chlorine dioxide can be further ozonated to chlorate ion. Alternatively, chlorite ion can be directly oxidized to chlorate ion (32,33,34).

$$2\ NaClO_2 + O_3 + H_2O \rightarrow 2\ NaOH + 2\ ClO_2 + O_2$$

$$2\ ClO_2 + O_3 + H_2O \rightarrow 2\ ClO_3^- + O_2 + 2H^+$$

$$NaClO_2 + O_3 \rightarrow NaClO_3 + O_2$$

If conditions could be found such that each reaction was quantitative and stopped at the desired intermediate oxidation state, then these three reactions could form the basis for analytical methods for ozone determination (35).

The stoichiometry of the reaction between chlorite ion and ozone was studied by measuring the chlorine dioxide formation as a function of the chlorite ion/ozone ratio, the stirring rate of the solution, and the pH.

In a series of experiments using constant aliquots of an ozone solution stabilized by acidification to pH 4, chlorine dioxide production increased as the chlorite ion concentration increased. As shown in Table 25, increasing the initial chlorite ion concentration from 1.22×10^{-2} M to 1.69×10^{-2} M, a 39% increase, caused a 34% increase in the chlorine dioxide formation. This large variation occurred even with the chlorite ion/ozone ratio greater than 60/1.

TABLE 25. EFFECT OF CHLORITE ION CONCENTRATION ON CHLORINE DIOXIDE FORMATION

$[ClO_2^-]$ M	$[ClO_2]$ M x 10^5
3.82 x 10-4	6.15
2.31×10^{-3}	6.52
7.48×10^{-3}	6.64
1.22×10^{-2}	7.28
1.69×10^{-2}	9.72

The rate of stirring during ozone addition to the chlorite ion-acetate buffer also affected the amount of chlorine dioxide produced. With a constant ozone sample and a constant chlorite ion concentration of 1.69×10^{-2} M, chlorine dioxide production decreased 18%, from 9.72×10^{-5} M to 8.08×10^{-5} M, with a decrease in the rate of stirring.

The increase in chlorine dioxide formation with an increase in chlorite ion concentration and with an increase in rate of stirring suggest that the chlorine dioxide is reacting with the ozone.

The pH of the chlorite ion-acetate buffer solution also had an effect on the chlorine dioxide formation. Injection of an ozone sample into a 1×10^{-3} M acetate buffer at pH 4.3 containing 1.69×10^{-2} M chlorite ion produced 18% more chlorine dioxide than injection of an equivalent ozone sample into 1×10^{-3} M acetate buffer at pH 5.3 containing 1.69×10^{-2} M chlorite ion. (Table 26).

TABLE 26. EFFECT OF pH ON CHLORINE DIOXIDE FORMATION

pH*	$[ClO_2]$ M
4.3	1.568×10^{-4}
5.3	1.328×10^{-4}

* 1×10^{-3} M acetate buffer, 1.69×10^{-2} M chlorite ion

Thermodynamically, chlorite ion can disproportionate to chlorine dioxide and oxygen according to the following equation:

$$6\ HClO_2 \rightarrow 4\ ClO_2 + O_2 + 2\ H_2O + 2\ Cl^- + 2\ H^+$$

At room temperature and at pH greater than two, disproportionation is usually negligible (36). However, ionic strength and buffer concentration were found to affect the stability of the chlorite ion in solution. As shown in Table 27, in 2×10^{-1} M acetate buffers at pH 4 and pH 5, 1.62×10^{-2} M chlorite ion decomposes to chlorine dioxide as measured by the increase in absorbance at 358.5 nm. When the buffer concentration is decreased to 1×10^{-3} M, chlorite ion is stable at pH 4 and pH 5.

TABLE 27. DECOMPOSITION OF CHLORITE ION IN 2 x 10^{-1} M ACETATE BUFFER

pH 4		pH 5	
time sec.	Abs 358.5 nm	time sec.	Abs 358.5 nm
0	0.068	0	0.068
80	0.075	80	0.069
160	0.084	160	0.071
240	0.093	240	0.074
320	0.102	--	--
400	0.111	--	--
480	0.121	--	--
560	0.132	560	0.076

The direct reaction between ozone and chlorine dioxide was studied by measuring the decrease in chlorine dioxide after addition of ozone to 6.56 x 10^{-5} M chlorine dioxide in 1 x 10^{-3} M acetate buffer at pH 5.3. Under these conditions, there was an initial rapid consumption of chlorine dioxide followed by a much slower decrease (Table 28). When the initial chlorine dioxide concentration was raised to 6.00 x 10^{-4} M, only the fast reaction was observed. In this case, the chlorine dioxide titer was stable within ten seconds of mixing the ozone and chlorine dioxide.

TABLE 28. REACTION BETWEEN CHLORINE DIOXIDE AND OZONE, pH 5.3, 1 x 10^{-3} M ACETATE BUFFER

time sec.	$[ClO_2]$ M x 10^5
0	6.56
30	1.92
70	1.40
110	1.20
150	1.08
190	1.00
230	0.96
1000	0.92

Hydrogen peroxide, a decomposition product omnipresent in aqueous ozone solution, theoretically can reduce chlorine dioxide to chlorite ion.

$$2ClO_2 + H_2O_2 \rightarrow 2ClO_2^- + O_2 + 2H^+$$

To test this potential interference, an aliquot of 3.0 mg/L hydrogen peroxide was injected into a rapidly stirring solution of 6.128×10^{-4} M chlorine dioxide at pH 4.3 in 1×10^{-3} M acetate buffer and the decrease in chlorine dioxide with time was followed spectrophotometrically. The kinetic results, summarized in Table 29, show that the reaction was slow but measurable. About 0.0% and 0.5% of the initial chlorine dioxide had reacted after one minute and nine minutes respectively.

Chlorite ion was confirmed as the product of the reaction between chlorine dioxide and hydrogen peroxide by injecting ozone into chlorine dioxide dissolved in acetate buffer at pH 4.3 as in the above kinetic experiment. After twenty-four hours reaction, the chlorine dioxide was purged from the reaction mixture with nitrogen gas. The UV spectrum of the resulting solution had the absorption pattern characteristic of chlorite ion, thus confirming chlorite ion formation in the reduction of chlorine dioxide with hydrogen peroxide.

TABLE 29. REACTION BETWEEN CHLORINE DIOXIDE AND HYDROGEN PEROXIDE AT pH 4.3, 1×10^{-3} M ACETATE BUFFER

time sec.	$[ClO_2]$ M x 10^4
0	6.12
60	6.12
120	6.11
180	6.11
240	6.11
300	6.11
360	6.10
420	6.10
480	6.10
540	6.09
1000	6.09

Clearly careful control of experimental conditions is necessary for the chlorite ion-ozone reaction and for the chlorine dioxide-ozone reaction to be used as analytical methods for residual ozone. Conditions for the chlorite ion method were optimized at a chlorite ion:ozone ratio of at least 200:1, efficient mixing during ozone addition to chlorite ion, an acetate buffer concentration of 1×10^{-3} M at pH 4.3 and immediate reading of the absorbance of chlorine dioxide. The chlorine dioxide method requires an initial chlorine dioxide concentration of at least 6×10^{-4} M, an acetate buffer concentration of 1×10^{-3} M at pH 4.3, and immediate reading of the chlorine dioxide absorbance.

Using these experimental constraints, the chlorite ion method and the chlorine dioxide method were compared by the kinetic technique. Ozone concentrations were calculated assuming a stoichiometry of one ozone molecule per two chlorine dioxide molecules. Measurements were taken on an ozone solution stabilized by acidification to pH 4 with phosphoric acid. Ideally both methods should give identical ozone titers. However, the results summarized in Table 30 clearly show the chlorine dioxide reaction gives 34% higher ozone titers than the chlorite reaction.

TABLE 30. DETERMINATION OF RESIDUAL OZONE BY CHLORITE ION AND BY CHLORINE DIOXIDE

time sec.	chlorite ion mg/L O_3	chlorine dioxide mg/L O_3
51	11.4	—
216	—	17.1
427	11.8	—
585	—	15.4
780	13.3	—
928	—	16.3
1095	11.9	—

A kinetic comparison was also made with the chlorite ion method, the DPD method, and the arsenic(III) back titration method on purified water (Fig. 28) and on Oxford tap water (Fig. 29). Generally low residual ozone titers are obtained with the chlorite ion method and the difference among methods tends to increase with increasing ozone concentrations.

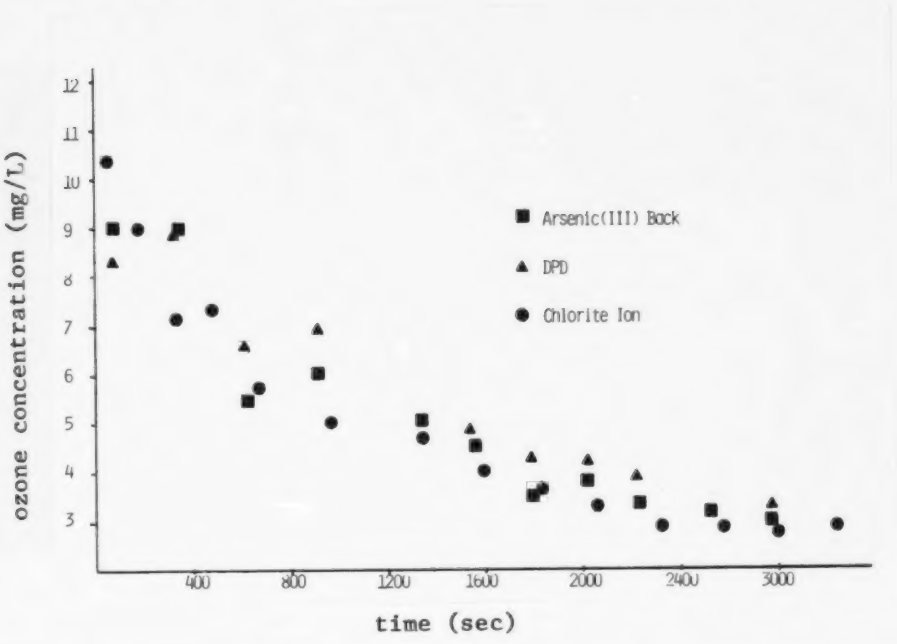

Figure 28. Comparison of As(III) Back, DPD, and Chlorite Ion in Purified Water.

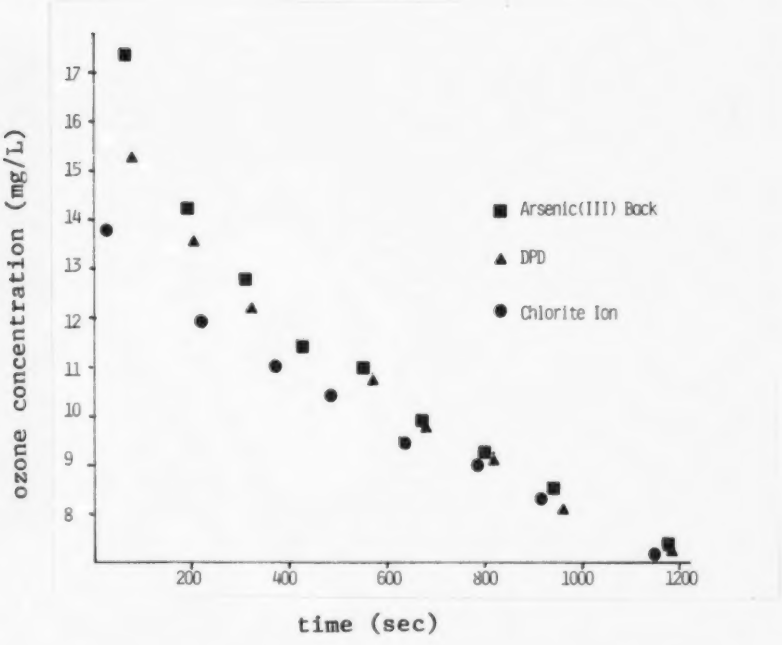

Figure 29. Comparison of As(III) Back, DPD, and Chlorite Ion in Tap Water.

All these results indicate that the reaction between chlorine dioxide and ozone is so fast that the chlorine dioxide formed in the chlorite ion method further reacts with ozone even in the presence of a two hundred fold excess of chlorite ion. Therefore, the chlorite ion method is eliminated as a practical analytical technique for residual ozone. Experience in handling chlorine dioxide solutions in the 1×10^{-3} to 1×10^{-4} M concentration range shows that 1% error in reproducibility is usual. This error, coupled with the low molar extinction coefficient and the need to generate the chlorine dioxide solution eliminate the chlorine dioxide method as a practical analytical technique for residual ozone. A mechanism for the reaction of ozone with chlorite ion is proposed below:

$$ClO_2^- + O_3 \rightarrow ClO_2 + O_3^-$$

$$O_3^- + H_2O \rightarrow OH\cdot + O_2 + OH^-$$

$$ClO_2^- + OH\cdot \rightarrow ClO_2 + OH^-$$

$$2\ ClO_2^- + O_3 + H_2O \rightarrow 2\ ClO_2 + O_2 + 2OH^-$$

Ozone reacts with chlorite ion to produce chlorine dioxide and ozonide ion (O_3^-) The ozonide ion rapidly reacts with water to produce the hydroxyl radical (OH•) which subsequently reacts with chlorite ion to produce a second molecule of chlorine dioxide. Thus, two successive one-electron transfers are probably involved in the reaction of ozone with chlorite ion to form chlorine dioxide. The stoichiometry of 1 ozone:2 chlorine dioxide is represented by the final equation.

Ozone can also react with chlorine dioxide in a parallel set of reactions to produce chlorate ion.

$$ClO_2 + O_3 + H_2O \rightarrow ClO_3^- + O_3^- + 2H^+$$

$$O_3^- + H_2O \rightarrow OH\cdot + O_2 + OH^-$$

$$ClO_2 + OH\cdot \rightarrow ClO_3^- + H^+$$

$$2\ ClO_2 + O_3 + H_2O \rightarrow 2\ ClO_3^- + O_2 + 2H^+$$

Chlorine dioxide competes with chlorite ion for ozone and hydroxyl radical and low results are observed using the chlorite ion method for residual ozone determinations.

Iron(II) Terpyridine Method

The iron(II) chelate complexes with substituted 1,10-phenanthrolines, 2,2'-bipyridines, and 2,2',2"-terpyridines are intensely colored and have high reduction potentials (37). Tris(1,10-phenanthroline)iron(II), commonly called ferroin, is a high potential redox indicator for titrations involving

strong oxidants. For example, ferroin has been used in titrations with cerium(IV) in the determination of iron, hydrogen peroxide, and arsenic(III). High precision and accuracy are obtained as the first excess of cerium(IV) oxidizes the ferroin to ferriin and changes the color from orange-red to very pale blue or colorless.

The oxidation of ferroin does not change the organic part of the complex. When ferroin is oxidized to ferriin, the phenanthroline ligands are not chemically altered. The ferrous atom gives up the electron and makes the ferroin-ferriin redox couple reversible.

The metal chelate complexes are also used for trace metal determinations. The iron(II) chelates form quantitatively at room temperature upon mixing ligand and iron(II) provided excess ligand and a suitable pH are employed. The large molar extinction coefficients of the iron(II) chelates makes these colorimetric procedures very sensitive.

Application of these complexes to residual ozone analysis was explored. Ideally ozone oxidizes the iron(II) complex to the iron(III) state; this causes a decrease in absorption that is proportional to the ozone concentration. Ferroin and 5-nitroferroin change from intense orange-red to pale blue on oxidation, tris (2,2'-bipyridine)iron(II) changes from intense red to faint blue on oxidation, and bis(2,2',2"-terpyridine)iron(II) changes from vivid violet to green on oxidation.

$$2\ Fe(Terpy)_2^{+2} + O_3 + 2H^+ \rightarrow 2\ Fe(Terpy)_2^{+3} + O_2 + H_2O$$

The wavelengths of maximum absorption of these four iron(II) complexes, their molar extinction coefficients (ε) and their reduction potentials (E°) are listed in Table 31.

TABLE 31. PROPERTIES OF IRON(II) CHELATES

complex	λmax	ε	E°(volts)
$Fe(phen)_3^{+2}$	510	11,000	1.112 [a]
$Fe(bipy)_3^{+2}$	522	8,650	1.069 [b]
$Fe(terpy)_2^{+2}$	552	11,500	1.076 [c]
$Fe(5\text{-}NO_2phen)_3^{+2}$	510	11,500	1.260 [c]

a) in 5×10^{-3} M H_2SO_4
b) in 1×10^{-2} M H_2SO_4
c) in 1×10^{-1} M H_2SO_4

A residual ozone analysis sensitive to the sub-mg/L range is indicated by the large molar extinction coefficients in the visible region. A very selective residual ozone analysis is indicated by the reduction potentials which are high compared with reduction potentials for the common reductants for ozone: arsenic(III), $E^\circ = 0.58v$ and iodide ion, $E^\circ = 0.53v$.

When freshly prepared ozone solutions chilled to 2°C are added to an indicator solution containing $Fe(terpy)_2^{+2}$, free terpyridine, and hydrochloric acid to adjust the pH between one and two, the absorption at 552 nm decreases with increasing amount of added ozone. Fig. 30 is a plot of the concentration of $Fe(terpy)_2^{+2}$ which was oxidized by ozone as a function of the concentration of added ozone. It appears that $Fe(terpy)_2^{+2}$ reacts with ozone stoichiometrically.

Substitution of $Fe(phen)_3^{+2}$ and free phenanthroline, and $Fe(bipy)_3^{+2}$ and free bipyridine for the $Fe(terpy)_2^{+2}$ and free terpyridine in the above experiment also leads to linear calibration curves for the reaction of these indicators with chilled fresh ozone solutions (Fig. 31 and 32).

The competitive reaction of ozone with $Fe(terpy)_2^{+2}$ and arsenic(III) was also examined to check stoichiometry. An aliquot of freshly prepared chilled ozone was mixed with a quantity of standard arsenic(III) solution that was insufficient to reduce all the ozone. This solution was then slowly stirred for a few seconds to allow the arsenic(III) to reduce the ozone according to the following equation.

$$O_3 + As^{+3} + 2H^+ \rightarrow As^{+5} + O_2 + H_2O$$

Excess $Fe(terpy)_2^{+2}$ was then added to reduce the remaining ozone according to the following equation.

$$2Fe(terpy)_2^{+2} + O_3 + 2H^+ \rightarrow 2Fe(terpy)_2^{+3} + O_2 + H_2O$$

Thus the relationship between the initial arsenic(III) concentration and the $Fe(terpy)_2^{+2}$ reacted with the ozone can be written

$$[O_3] = 2[Fe(terpy)_2^{+2}] + [As^{+3}]$$

and a plot of $[Fe(terpy)_2^{+2}]$ vs. $[As^{+3}]$ should be linear with a slope of 2. Fig. 33 is indeed linear with a slope of 2 and thus confirms the stoichiometry 1:2 of the ozone -$Fe(terpy)_2^{+2}$ reaction.

Some problems with instability of the oxidized indicators were encountered. When a fresh ozone solution was added to solutions of $Fe(phen)_3^{+2}$, $Fe(bipy)_3^{+2}$, and $Fe(terpy)_2^{+2}$ without addition of free ligand and without acid, only transient and incomplete bleaching occurred. The reappearance of the color was almost immediate. This was most probably due to the instability of the oxidized complexes, $Fe(phen)_3^{+3}$, $Fe(Bipy)_3^{+3}$ and $Fe(terpy)_2^{+3}$, under these conditions. Neither adjustment of the pH to one nor the addition of free ligand alone stabilized the oxidized complexes. The presence of both acid and ligand was essential.

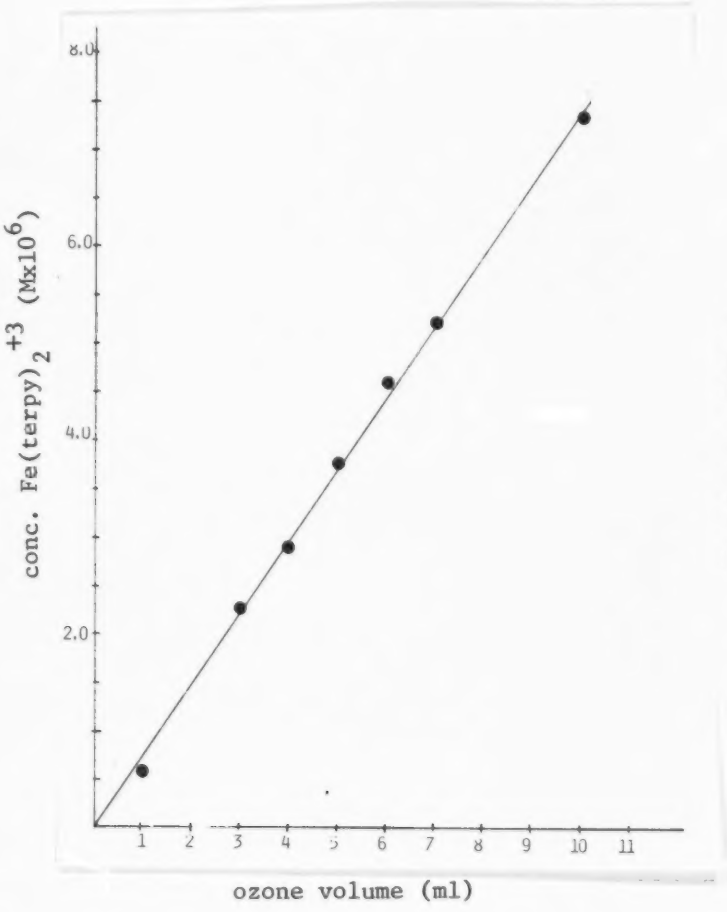

Figure 30. Calibration Curve for $Fe(terpy)_2^{+2}$.

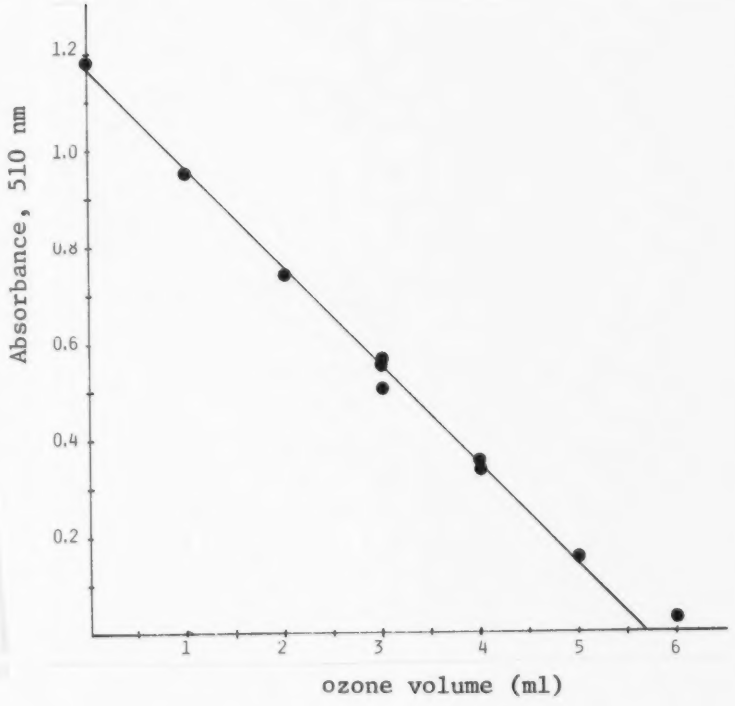

Figure 31. Calibration Curve for $Fe(phen)_3^{+2}$.

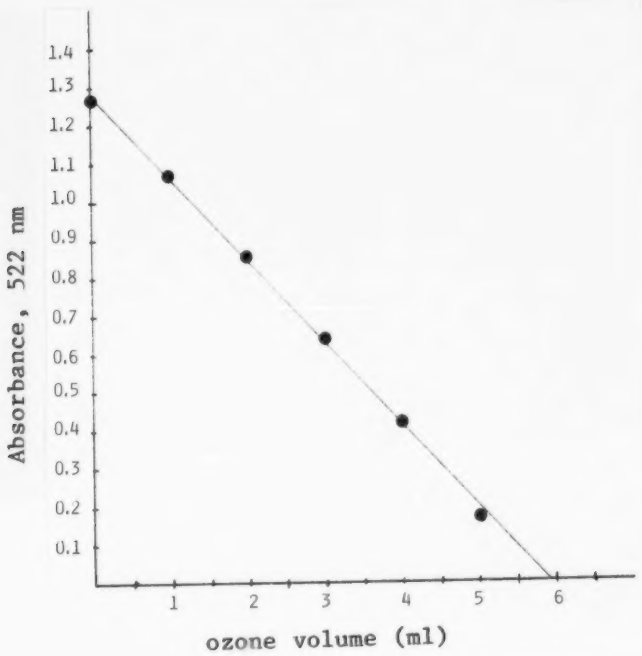

Figure 32. Calibration Curve for $Fe(bipy)_3^{+2}$.

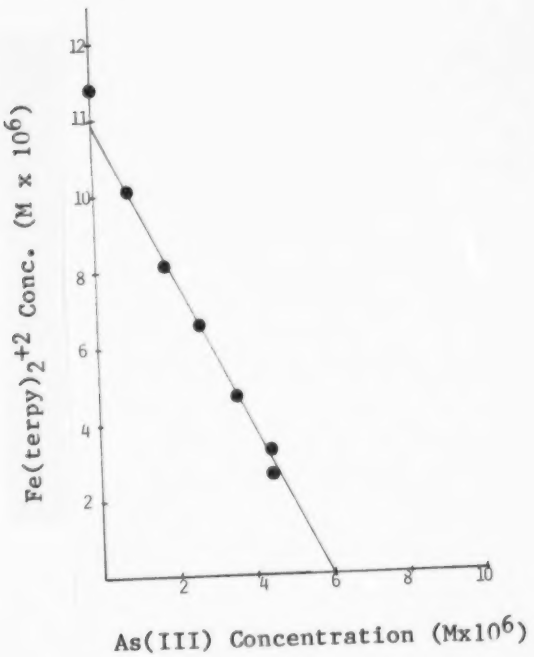

Figure 33. Competitive Reaction of Ozone with $Fe(terpy)_2^{+2}$ and As(III).

With $Fe(terpy)_2^{+2}$, the requirements were even more specific. Hydrochloric acid was the only acid observed to significantly stabilize the $Fe(terpy)_2^{+3}$ complex. Sulfuric acid, perchloric acid and phosphoric acid were ineffective. Sodium chloride in a neutral solution also failed to stabilize the decolorization.

The ozone decolorization of $Fe(terpy)_2^{+2}$ indicator solution containing excess terpyridine and hydrochloric acid, however, was dependant on the free terpyridine concentration. After ozone addition to standard $Fe(terpy)_2^{+2}$ indicator solution, an absorbance reading of 0.01818 was recorded. Addition of a few crystals of free terpyridine to this solution increased the absorbance reading by 43 percent. A second addition of solid terpyridine further increased the absorbance reading by 37 percent. Clearly the terpyridine is shifting complex equilibria and absorbance measurements may not reflect the true reductant concentration.

When $Fe(terpy)_2^{+2}$ indicator solutions were injected with ozone solutions which had been prepared by bubbling ozone through 20°C water for thirty minutes or longer, unstable absorbance readings resulted. This is in disagreement with the stable absorbance readings obtained with freshly prepared chilled ozone solutions. The absorbance increased with time but the rate of increase varied from ozone solution to ozone solution. Generally, low absorbance measurements increased the most rapidly with time. Table 32 shows some typical data for the percent increase in absorbance over ten minutes as a function of the percent indicator not oxidized. When ozone oxidized 95 percent of the indicator so that only 5 percent of the initial absorbance remained, the absorbance reading increased 64 percent in the first ten minutes following ozone addition. With 51 percent of the $Fe(terpy)_2^{+2}$ unoxidized, there was no steady increase in absorbance. Scattered readings above and below the initial value were obtained.

TABLE 32. STABILITY OF ABSORBANCE READING FOR $Fe(terpy)_2^{+2}$ METHOD

Abs after O_3 x 100	% increase/10 min.
100	stable
76	4
66	13
51	scatter
17	15
7	33
5	64

Thus, it appears that a decomposition product of ozone present in the aged solution must be causing the instability. A prime suspect is hydrogen peroxide. Therefore, in order to test the hypothesis that hydrogen peroxide is the cause of the absorbance increase, and also to test whether initial absorbance readings accurately reflect oxidant concentration, the cerium(IV) oxidation of the iron(II) complexes was studied. In this system, cerium(IV), a standard reagent in 1 M H_2SO_4, is free from any extraneous decomposition impurities that might be present in ozone solutions. Following cerium(IV) oxidation of $Fe(phen)_3^{+2}$, $Fe(bipy)_3^{+2}$, and $Fe(terpy)_2^{+2}$ in solutions at pH one to two containing excess free ligand stable absorbance readings were obtained. Addition of hydrogen peroxide to these cerium(IV) oxidized solutions produced a 30 to 40 percent increase in absorbance within ten minutes. This rapid increase in absorbance was also observed following addition of hydrogen peroxide to indicator solutions already decolorized by ozone. If the hydrogen peroxide was added to the indicator solution prior to oxidation, then ozone addition caused only incomplete and transient decolorization. These results support the argument that hydrogen peroxide, or some other decomposition product, is responsible for the increasing absorbance readings following ozone oxidation of the iron(II) complexes.

Comparison of the experimentally determined concentration of $Fe(phen)_3^{+2}$, $Fe(bipy)_3^{+2}$, and $Fe(terpy)_2^{+2}$ remaining unoxidized following standard cerium(IV) addition with the theoretical concentration based on the amount of cerium(IV) added revealed that all experimental values were high. The discrepency increased as the cerium(IV) concentration increased (Table 33). These results imply that use of these iron(II) complexes as quantitative redox reagents yields low oxidant titers.

TABLE 33. OXIDATION OF IRON(II) COMPLEXES BY CERIUM(IV)

Reductant	$[Reductant]_{exp.} \times 10$	$[Reductant]_{theor} \times 10^6$
$Fe(phen)_3^{+2}$	7.98	1.25
	5.80	1.25
	11.3	7.25
$Fe(bipy)_3^{+2}$	6.19	1.70
$Fe(terpy)_2^{+2}$	4.00	1.40
	5.89	1.40

The kinetic comparison of residual ozone in purified water by the arsenic(III) direct oxidation method and the $Fe(terpy)_2^{+2}$ method confirms the low ozone titers with the $Fe(terpy)_2^{+2}$ method (29). Ozone titers were consistently 55 percent lower with the $Fe(terpy)_2^{+2}$ method than with the arsenic(III) direct oxidation method. (Fig. 34). Similarly in a kinetic comparison of residual ozone in purified water with the arsenic(III) back titration method, the DPD method, and the $Fe(terpy)_2^{+2}$ method, the $Fe(terpy)_2^{+2}$ method gives low results. (Fig. 35).

This large discrepency in residual ozone levels is probably caused by a complex combination of shifting equilibria, unstable complexes, hydrogen peroxide interference, and reaction of ozone with ligand or hydrochloric acid. Whatever the cause, however, the final conclusion must be that the iron(II) complexes are not suitable redox reagents for quantitative ozone analysis.

As mentioned earlier in Table 31, the iron(II) 5-nitrophenanthroline complex has a reduction potential of 1.26 volts and thus is a stronger oxidant than the above three iron(II) complexes. When used as a reductant for both ozone and cerium(IV), high unstable absorbance readings resulted. The absorbance decreased steadily with time. A decrease of 20 to 50 percent within six minutes was typical.

The ruthenium complexes of Table 34 were also examined as potential reductants for ozone. The ruthenium(II) complexes are stronger oxidants and stronger absorbers than the corresponding iron(II) complexes. Reportedly, they are more stable in the ruthenium(II) and ruthenium(III) state than the iron(II) and iron(III) complexes (37). If the instability problem can be overcome, then they offer a very selective and very sensitive method for residual ozone analysis. Unlike the iron analogues, these ruthenium complexes must be separately synthesized and isolated prior to use.

TABLE 34. PROPERTIES OF RUTHENIUM(II) COMPLEXES

complex	λnm	ε	E° volts
$Ru(phen)_3^{+2}$	447	19000	1.26 [a]
$Ru(bipy)_3^{+2}$	452	14600	1.26 [a]
$Ru(terpy)_2^{+2}$	473	16200	1.28 [b]
$Ru(5\text{-}NO_2\text{-}phen)_3^{+2}$	449	20000	1.46

[a] in 1 M H_2SO_4 [b] in 1 x 10^{-1} M H_2SO_4

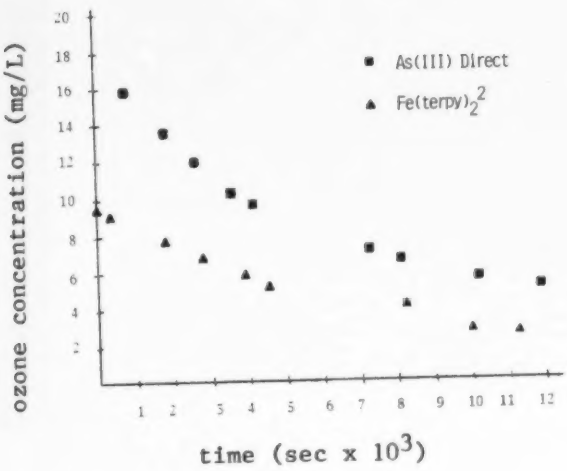

Figure 34. Comparison of As(III) Direct and $Fe(terpy)_2^{+2}$ in Purified Water.

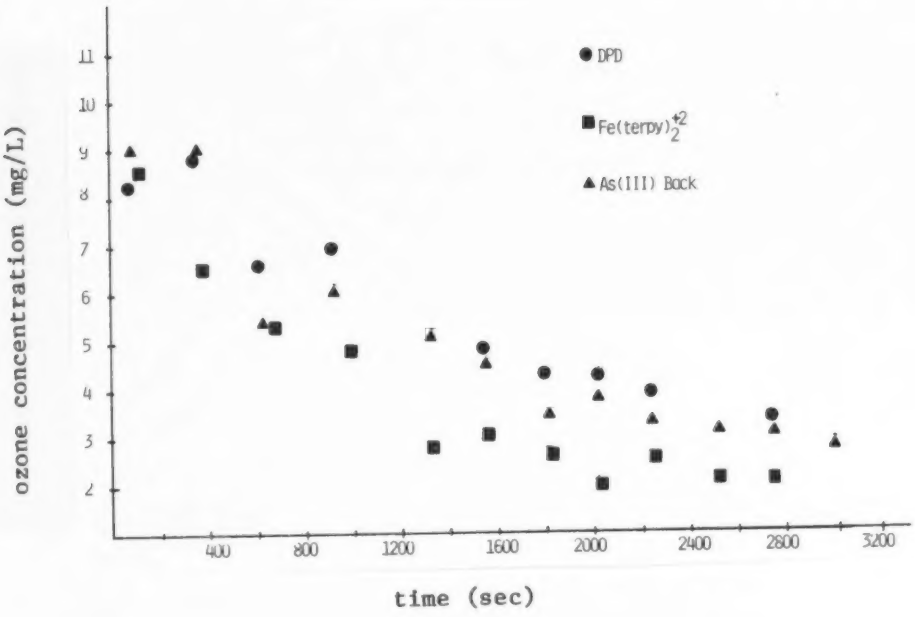

Figure 35. Comparison of DPD, $Fe(terpy)_2^{+2}$, and As(III) Back in Purified Water.

For each of the four complexes, excess cerium(IV) was required for decolorization and after decolorization, the absorbance due to the ruthenium(II) complex increased rapidly with time. Addition of ozone to the ruthenium(II) complexes produced no discernable decolorization. Clearly, these complexes also are unsuitable as reductants for aqueous ozone.

Iodate Method

The classical method of residual ozone analysis in water is based on the oxidation of potassium iodide to iodine in the presence of excess iodide ion. The triiodide ion formed is more stable in water than the ozone but the iodometric methods are still susceptible to error due to iodine volatility, air oxidation of iodide ion, hydrogen peroxide formation and its subsequent oxidation of iodide ion, and hypoiodite ion and iodate ion formation. These problems are all discussed in detail earlier in this report. Numerous modifications in the reaction conditions and titration techniques for the ozone-iodide based methods have been proposed in order to minimize the above problems.

The iodate method was designed to capitalize on the great stability of the iodate ion and on the capability of differential pulse polarography (DPP) to accurately detect sub-mg/L iodate ion concentrations (24). In this volumetric variation, ozone is added to a potassium iodide solution buffered at pH 8-9. After five minutes, the solution is adjusted to pH 13-14 with sodium hydroxide and allowed to react for at least one hour. An aliquot is then analyzed for iodate ion by differential pulse polarography. The iodate ion solution, in contrast to solutions of iodine and triiodide ion, is stable for prolonged periods, is not susceptible to air oxidation and is not volatile.

Theoretically the ozone reacts with the iodide ion to form a mixture of iodine and iodate ion (2).

$$O_3 + 2I^- + 2H^+ \rightarrow I_2 + O_2 + H_2O$$

$$3O_3 + I^- \rightarrow 3O_2 + IO_3^-$$

$$5O_3 + I_2 + H_2O \rightarrow 5O_2 + 2IO_3^- + 2H^+$$

As the pH is increased above nine, the iodine undergoes disproportionation to form hypoiodite ion and iodide ion. The hypoiodite ion then undergoes further disproportionation to form iodate ion and iodide ion.

$$I_2 + 2OH^- \rightarrow IO^- + H_2O + I^-$$

$$3IO^- \rightarrow 2I^- + IO_3^-$$

Thus, theoretically the ozone oxidation of iodide ion can be controlled to produce iodate ion quantitatively. Regardless of whether the iodate ion is formed directly by ozone oxidation of iodide ion or indirectly by

disproportionation of iodine formed from ozone oxidation of iodide ion, three moles of ozone produce one mole of iodate ion.

The Iodate method and the Iodometric method were compared with the kinetic technique (24). This comparison is unique in this ozone work because the uncertainty due to sampling variations is eliminated. The identical ozone-iodide ion sample is analyzed by the two methods. The ozone sample is injected into an iodide ion solution at pH 8. The solution is diluted to standard volume and one aliquot is immediately added to a flask containing excess standard sodium thiosulfate solution. The pH is adjusted to pH 2 with 6 M sulfuric acid and after five minutes the excess thiosulfate ion is back titrated with standard iodine to an amperometric end-point. A second aliquot of the ozone-iodide ion reaction solution is adjusted to pH 13 and after one hour the sample is analyzed for iodate ion by differential pulse polarography. In this manner, a very accurate comparison between the Iodometric method and the iodate method is possible. Table 35 lists the results of the kinetic comparison.

Utilizing the first seven data points for the Iodometric method and all data points for the Iodate method, the best fit kinetic model was obtained for each method. From these equations describing the smoothed time-concentration curves for each method, the ozone concentrations were calculated and compared. The two methods were indistinguishable with these calculated concentrations.

TABLE 35. KINETIC COMPARISON OF IODOMETRIC AND IODATE METHODS

Ozone Concentration mg/L		
Iodometric	Iodate	Calculated
9.03	6.72	8.98
6.35	6.44	6.13
4.49	4.64	4.61
3.59	3.67	3.65
2.24	2.33	2.44
1.59	1.66	1.63
1.48	1.23	1.39
0.62	0.50	0.51
0.27	0.49	0.50
--	0.43	0.45
--	0.36	0.40

The experimental values, however, do reveal potential differences between the methods over the concentration range studied. The experimental residual ozone levels determined by the Iodometric method agreed within eight percent of the calculated ozone concentrations for residual ozone levels above 1.48 mg/L. Below this level, however, differences between experimental and calculated concentrations of +22 percent and -46 percent were found. Clearly the Iodometric method is unreliable below the one mg/L ozone level.

In contrast, the iodate method experimental ozone values showed maximum difference from the calculated values at the high ozone concentration. Experimental values below one mg/L were within ten percent of the calculated values. Generally the error in the iodate method tended to low experimental ozone titers. Since the need in ozone methodology is in the low ozone range, and since the iodate method seems promising, conditions for the iodate method were varied in an attempt to insure accuracy over a wide ozone concentration.

Iodate ion gives a well defined polarographic reduction wave in alkaline solution. The half-wave potential is practically independent of pH above pH 8, but an increase in sensitivity is noted with increasing pH (30). Iodate ion concentrations as low as 2.3×10^{-7} M can be measured with differential pulse polarography (31). This value corresponds to a detection limit of 0.004 mg/L ozone.

The accuracy of the iodate method depends on the quantitative conversion of iodide ion and iodine to iodate ion. The iodine conversion is readily evaluated by measuring iodate ion formation from the disproportionation of aliquots of standard iodine solution. Initial experiments with the conditions used in the kinetic comparison revealed low iodine-iodate ion conversions. Therefore, a systematic study was carried out to search for suitable conditions. Variations in pH, buffer, iodide ion, reaction time and reaction temperature were studied.

Table 36 shows the effect of hydroxide ion concentration on the amount of iodate ion produced from the disproportionation of iodine. The percent reaction initially increased with hydroxide ion concentration, but further increases in hydroxide ion concentration inhibited iodine disproportionation to iodate ion. Table 36 suggests an optimum hydroxide ion concentration of 0.1 to 0.25 M.

A study of the effect of carbonate ion and phosphate ion on the disproportionation of iodine suggests that carbonate ion does have a slight positive effect. (Table 37).

The carbonate ion concentration was varied to optimize its catalytic effect (Table 38). The positive effect maximizes at a carbonate ion concentration of 0.4 - 0.5 M.

Using the optimum conditions defined by the previous experiments, the effect of potassium iodide concentration on the disproportionation of iodine was studied. The results in Table 39 show only a slight positive iodide ion effect up to concentrations of 0.16 g/ml. Higher iodide ion levels decreased iodate ion formation due to a shift of the hypoiodite ion-iodide ion equilibrium towards iodine.

TABLE 36. EFFECT OF HYDROXIDE ION ON THE DISPROPORTIONATION OF IODINE TO IODATE ION

$[OH^-]$[a] M	$[IO_3^-]$found M x 10^6	% Reaction[b]
0.05	0.700	44.2
0.10	0.923	58.2
0.25	0.848	53.5
0.50	0.736	46.5
1.00	0.592	37.3
3.00	0.228	14.4

[a] 25 ml reaction volume, 4 g KI, 80°C, 1 hr.

[b] $[IO_3^-]_{theoretical} = 1.58 \times 10^{-6}$ M

TABLE 37. EFFECT OF CARBONATE AND PHOSPHATE IONS ON THE DISPROPORTIONATION OF IODINE

Anion	$[IO_3^-]$found M x 10^6	% Reaction [b]
0.1 M $CO_3^=$ [a]	0.871	55.0
0.1 M $PO_4^=$ [a]	0.674	43.5
control [a]	0.748	47.2

[a] 25 ml reaction volume, 4 g KI, $[OH^-]$ = 0.25 M, 80°C, 1 hr.

[b] $[IO_3^-]_{theoretical} = 1.58 \times 10^{-6}$ M

TABLE 38. EFFECT OF CARBONATE ION ON THE DISPROPORTIONATION OF IODINE

$[CO_3^{=}]$ [a]	$[IO_3^-]$found	% Reaction [b]
M	M x 10^6	
0.138	1.04	63.6
0.276	1.01	62.2
0.414	1.15	70.5
0.551	1.16	70.9
0.689	1.10	67.5

[a] 25 ml reaction volume, 4 g KI, $[OH^-]$ = 0.26 M, 80°C, 1 hr.

[b] $[IO_3^-]_{theoretical}$ = 1.63 x 10^{-6} M

TABLE 39. EFFECT OF IODIDE ION ON THE DISPROPORTIONATION OF IODINE

[KI][a]	$[IO_3^-]$found	% Reaction[b]
g/ml	M x 10^6	
0.010	1.16	66.0
0.020	1.18	67.2
0.040	1.19	67.8
0.080	1.26	71.3
0.16	1.20	68.4
0.32	1.08	61.3
0.48[c]	0.958	54.5
0.64[c]	0.860	48.9
0.80[c]	0.715	40.6

[a] 25 ml reaction volume, $[OH^-]$ = 0.26 M, $[CO_3^{=}]$ = 0.41 M, 80°C, 1 hr.

[b] $[IO_3^-]_{theoretical}$ = 1.75 x 10^{-6} M

[c] iodine color present during reaction, but not after 1 hr. of reaction

Finally, the reaction time at 80°C was varied. As shown in Table 40, increasing the reaction time beyond two hours did not increase the percentage of iodate ion formed. Only a maximum of 82.2 percent of theoretical could be detected.

TABLE 40. EFFECT OF REACTION TIME ON THE DISPROPORTIONATION OF IODINE

Reaction time[a] hr.	$[IO_3^-]$found M x 10^6	% Reaction[b]
1	1.20	68.6
2	1.44	82.2
3	1.34	76.5
4	1.41	80.5
5	1.42	80.7
6	1.33	75.9

[a] 25 ml reaction volume, $[OH^-]$ = 0.26 M, $[CO_3^=]$ = 0.41, 4 g KI, 80°C

[b] $[IO_3^-]_{theoretical} = 1.75 \times 10^{-6}$ M

The incomplete conversion of iodine to iodate ion is unacceptable. Souchay reports that the half-life for the conversion of 1.2 x 10-2 M hypoiodite ion to iodate ion is five minutes in 0.2 M potassium hydroxide and that the rate law for hypoiodite ion disproportionation is approximately second order with respect to hypoiodite ion (38). Therefore, as the hypoiodite ion concentration decreases, the half-life increases with the reciprocal of the hypoiodite ion concentration. Since the ozone oxidation of iodide ion produces both iodine and iodate ion and since the iodine must be quantitatively disproportionated to iodate ion, this inability to achieve quantitative conversion of iodine to iodate ion eliminates the iodate method for residual ozone analyses.

Cerium Method

The cerium(III)-cerium(IV) couple could form the chemical basis for a very specific analytical procedure for residual ozone. Any ambiguity with respect to oxidation states and on reaction stoichiometry is minimized due to the one electron change involved in the cerium(III)-cerium(IV) couple. Great selectivity is promised by the high reduction potential for the cerium(III)-cerium(IV) couple in strongly acidic solutions. In addition, the acidic reaction medium, totally free of organic ligands and reagents, should minimize ozone decomposition prior to reduction by cerium(III).

$$Ce^{+4} + 1e^- \rightarrow Ce^{+3}$$

E° = 1.44 in 1 M H_2SO_4

E° = 1.61 in 1 M HNO_3

E° = 1.70 in 1 M $HClO_4$

As seen above, the reaction potential varies with the acid medium. This is caused by the complexation of cerium ions with anions and water to form stable complexes that are the true oxidized and reduced species.

The reactions of interest in the potential cerium method are first the ozone oxidation of cerium(III) to cerium(IV) and second the quantitative determination of the cerium(IV) produced.

$$O_3 + 2\ Ce^{+3} + 2H^+ \rightarrow O_2 + 2\ Ce^{+4} + H_2O$$

Because of the higher reduction potentials, perchloric acid and nitric acid solutions of cerium(III) promise more selectivity than sulfuric acid solutions. However, solutions of cerium(IV) in nitric acid and perchloric acid slowly attack water and decrease in normality about one percent during storage for one month. Sulfuric acid solutions of cerium(IV) are constant in titer for years (39). This increased stability of cerium(IV) offers a very stable ozone titer and makes sulfuric acid the medium of choice. The cerium(IV) could be detected electrochemically or by a variety of other well defined properties of cerium(IV) itself. For convenience and overlap with other experimental methods concurrently being investigated the decolorization of ferroin was utilized here.

$$Ce^{+4} + Fe(phen)_3^{+2} \rightarrow Ce^{+3} + Fe(phen)_3^{+3}$$

red-orange pale blue - colorless

There is one known complication. Hydrogen peroxide quantitatively reduces cerium(IV) to cerium(III) as shown in the following equation (39).

$$2\ Ce^{+4} + H_2O_2 \rightarrow 2\ Ce^{+3} + O_2 + 2H^+$$

Therefore, the ozone concentration determined by means of the direct reaction between cerium(III) and ozone would be low due to the simultaneous reduction of the cerium(IV) product by hydrogen peroxide. A correction for this error can be made by measuring the decrease in cerium(IV) concentration caused by reaction of standard cerium(IV) solution with an ozonated water sample purged of the volatile ozone. This technique, then, allows the simultaneous determination of both ozone and hydrogen peroxide in residual ozone samples. If this correction is too tedious for routine use, then this cerium method could still be valuable as a new calibration procedure independent of iodimetry.

The cerium method successfully converted the unstable, volatile ozone solution to a stable, non-volatile cerium(IV) solution which repeatedly produced the same ozone titer when sampled and reacted with ferroin over a period of twenty-four hours. This stability is matched only by the arsenic(III) direct oxidation method and by the indigo method.

Commercial hydrogen peroxide diluted to 1.7×10^{-5} M gave a linear calibration curve when analyzed by cerium(IV) reduction with ferroin detection as shown in Fig. 36. Thus, this promised a convenient analytical method for

the non-volatile ozone solution impurities which are weaker oxidants than cerium(IV). Values in the 0.20 to 0.40 mg/L range were found by this method for the hydrogen peroxide levels in purged ozone solutions.

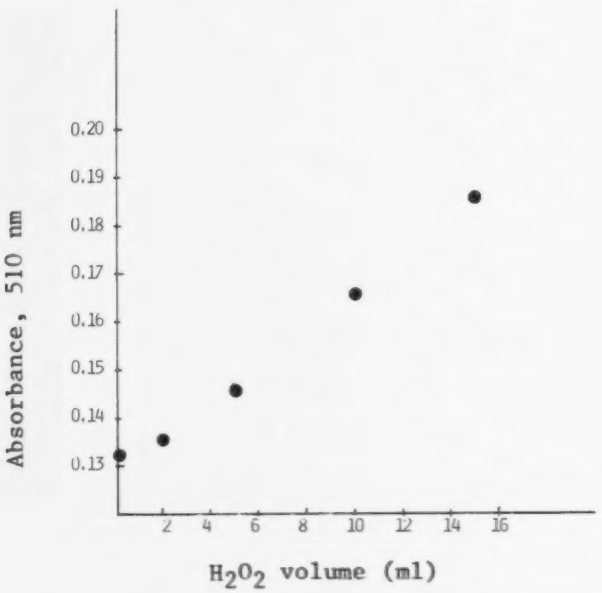

Figure 36. Hydrogen Peroxide Analysis by the Cerium Method.

The cerium method, the DPD method, and the arsenic(III) back titration method were used to follow ozone decay in purified water and in Oxford tap water. (Fig. 37 and 38). The decay curves for ozone in purified water defined by each of the three methods show considerable scatter. This scatter is typical for the DPD method and the arsenic(III) back titration method which both involve ozone reactions at neutral pH. The scatter was unexpected for the cerium method because in analogy with the indigo method, the strongly acidic reaction medium was expected to minimize ozone decay prior to reduction with cerium(III).

Assuming the problem lies in the Ce(III)-ozone reaction and not in the Ce(IV)-ferroin reaction, this erratic scatter eliminates the cerium method as a viable reference/calibration procedure for residual ozone.

In Oxford tap water, smooth decay curves are traced by the DPD method and by the arsenic(III) back titration methods. Very low and very scattered residual ozone concentrations are measured by the cerium method. This could be caused by the reaction of the produced Ce(IV) with metal ions and other organic impurities. Whatever the reason, the cerium method clearly fails as an analytical method for residual ozone determination.

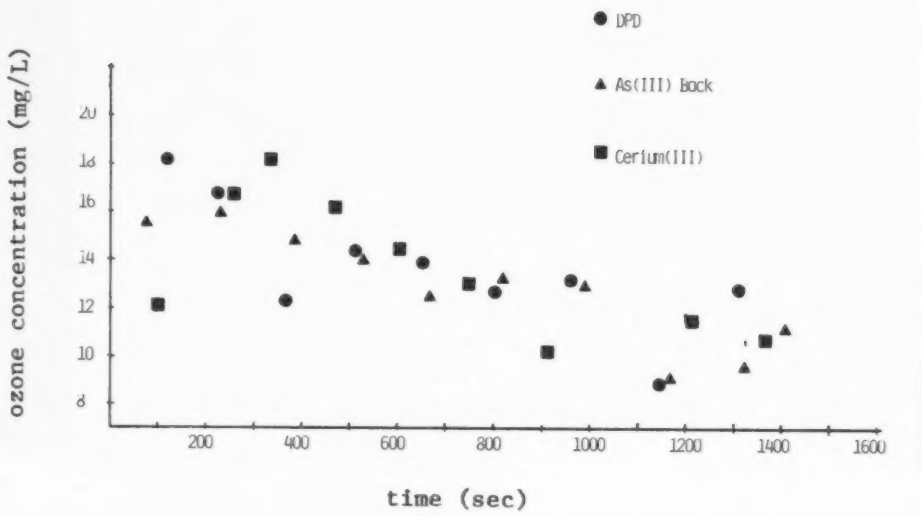

Figure 37. Comparison of DPD, As(III) Back, and Cerium(III) in Purified Water.

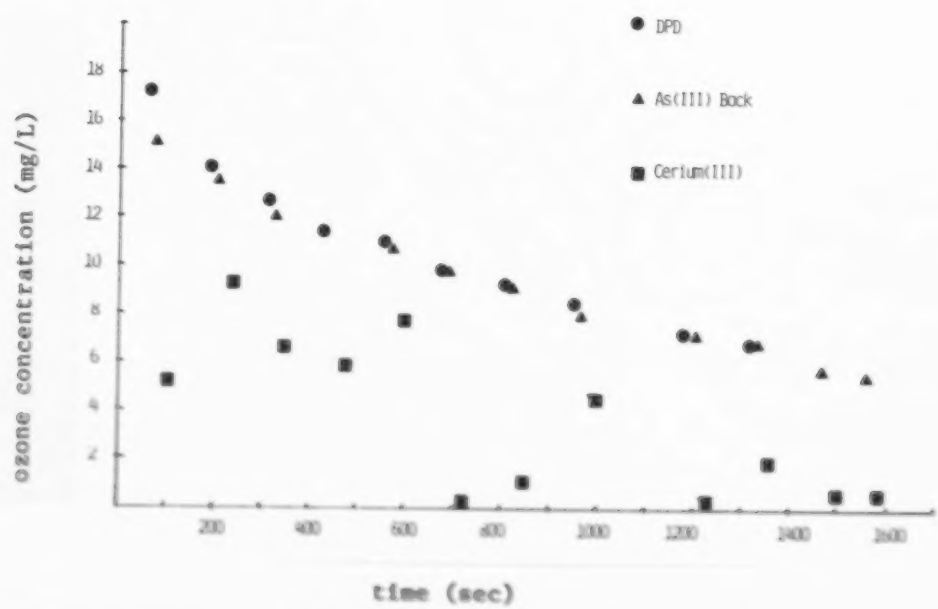

Figure 38. Comparison of DPD, As(III) Back, and Cerium(III) in Tap Water.

REFERENCES

1. Symons, J. M., "Ozone, Chlorine Dioxide and Chloramines as Alternatives to Chlorine for Disinfection of Drinking Water", presented at the Second Conference on Water Chlorination, Gatlinburg, Tenn., November 1977.

2. Manley, T. C. and Niegouski, S. J. in "Kirk-Othmer: Encyclopedia of Chemical Technology", Vol. 14, 2nd ed.; Mark, H. F., McKetta, J. J. Jr., Othmer, D. F. Eds.; Interscience: New York, 1967; pp 410-432.

3. Smart, R. B., Lowery, J. H., Mancy, K. H., Envir. Sci. and Tech., 13, 89-92 (1979).

4. Bader, H., Hoigné, J., Water Res., 15, 449-456 (1981).

5. Stanley, J. H., Johnson, J. D., Anal. Chem., 51, 2144-2147 (1979).

6. G. Gordon and J. Grunwell, "Comparison of Analytical Methods for Residual Ozone", Proceedings of the Second National Symposium on Municipal Waste Water Disinfection, in press (1982).

7. "Standard Methods for the Examination of Water and Waste Water", American Public Health Association, 14th ed., American Public Health Association, Washington, D.C., 1975.

8. Saltzman, B.E. and Gilbert, N., Anal. Chem., 31, 1914-1920 (1959).

9. Byers, D.H. and Saltzman, B.E., "Ozone Chemistry and Technology", Advances in Chem. Series, Vol. 21, pp. 93-101 (1959).

10. Ingols, R.S., Fetner, R.H., and Eberhardt, W.H., "Ozone Chemistry and Technology", Advances in Chem. Series, Vol. 21, pp. 102-107 (1959).

11. Boyd, A. W., Willis, C., Cyr, R., Anal. Chem., 42, 670 (1970).

12. Kopszynski, S. L., Bufalini, J. J., Anal. Chem., 43, 1126-1127 (1971).

13. Hodgeson, A., Baumgardner, R.E., Martin, B.E., and Rehme, K.A., Anal. Chem., 43, 1123-1126 (1971).

14. Dietz, R.N., Pruzansky, J., Smith, J.D., Anal. Chem., 45, 402-404 (1973).

15. Flamm, D. L., Envir. Sci. and Tech., 11, 978-983 (1977).

16. Parry, E. P., Hern, D. H., Envir. Sci. and Tech., 7, 65-66 (1973).

17. Bergshoeff, G., Lanting, R.W., Prop, J.M.G., and Reynders, H.F.R., Anal. Chem., 52, 541-456 (1980).

18. Sullivan, D. E., Hall, L. C., D'Ambrosi, M., Roth, J. A., Ozone Sci. and Eng., 2, 183-193 (1980).

19. Palin, A. T., Water and Water Eng., July, 271-277 (1953).

20. Kilpatrick, M. L., Herrick, C. D., J. Am. Chem. Soc., 78, 1784-1889 (1965).

21. Bader, H., Hoigne´, J., Water Res., 10, 377-386 (1976).

22. Bahnemann, D., Hart, E. J., J. Phys. Chem., 86, 252-255 (1982).

23. Forni, L., Bahnemann, D., Hart, E. J., J. Phys. Chem., 86, 255-259 (1982).

24. Benga, J., Dissertation for Ph.D., Miami University, 1980.

25. Peleg, M., Water Res., 10, 331-365 (1976).

26. Staehelin, J., Hoigne´, J., 5th World Congress International Ozone Assoc., Proceedings in Press (1981).

27. Gordon, G., Kieffer, R. G., Rosenblatt, D. H., "The Chemistry of Chlorine Dioxide", Progress in Inorganic Chemistry, S. L. Lippard, Eds., Vol. 15 (New York, Wiley-Interscience Pub., 1972), p. 209.

28. Braddock, J. N., Meyer, T. J., J. Am. Chem. Soc., 95, 3158 (1973).

29. Cohen, H., Dissertation for M.S., Miami University, 1981.

30. Kolthoff, I. M., Lingane, J. J., "Polarography", 2nd ed., Interscience: New York, 1952.

31. Herring, J. R., Liss, P. S., Deep-Sea Res., 21, 777-783 (1974).

32. Masschelein, W. J., Chlorine Dioxide Chemistry and Environmental Impact of Oxychlorine Compounds, (Ann Arbor: Ann Arbor Publishers, Inc., 1979).

33. Kolle, W., Vom Vasser, 35, 367 (1968).

34. Schack, C. J., Christe, K. O., Inorg. Chem., 13, 2378 (1974).

35. Emerich, D., Dissertation for Ph.D., Miami University, 1981.

36. Kieffer, R. G., Gordon, G., Inorg. Chem., 7, 235 (1968).

37. Schlit, A., "Analytical Applications of 1,10-Phenanthroline and Related Compounds", International Series of Monographs in Analytical Chemistry, Vol. 32, Pergamon Press, New York, 1969.

38. Souchay, P., Anal. Chim. Acta, 2, 17-29 (1948).

39. Vogel, A. I., "A Textbook of Quantitative Inorganic Analysis", 4th ed., Longman: London, 1978.